4-2007

Biochemical Characterization of Disease-Causing Mutation in N-Terminal Wilson Protein Domain Six

Patrick Ochieng

BIOCHEMICAL CHARACTERIZATION OF DISEASE-CAUSING MUTATION IN N-TERMINAL WILSON PROTEIN DOMAIN SIX

by

Patrick Ochieng

A Thesis
Submitted to the
Faculty of The Graduate College
in partial fulfillment of the
requirements for the
Degree of Master of Science
Department of Chemistry

Western Michigan University
Kalamazoo, Michigan
April 2007

ACKNOWLEDGEMENTS

First, I want to thank the Chemistry Department of Western Michigan University for giving me the opportunity to pursue my graduate studies in chemistry. I also want to thank my research advisor Dr. David Huffman, for his continuous support during my masters program. Dr. Huffman particularly introduced me to competitive research in Western Michigan University by involving me in the Wilson disease project. Through his NIH grant, he was able to support me and my research for six months while at the Centre for Magnetic Resonance (CERM), Italy and also at Western Michigan University. Thanks also for the valuable corrections and suggestions he made on this thesis. I would also want to thank our collaborators at the University of Florence Italy, for the fellowship they awarded me to conduct part of this research in their magnificent NMR facility. Thanks to Prof. Ivano Bertini, Prof. Lucia Banci and Dr. Simone Ciofi-Baffoni for the mentorship they gave me while in CERM.

Besides my advisors, I would like to thank my thesis committee members; Dr. Sherine Obare and Dr. Dongil Lee for their support and availability in my committee meetings. Thanks also for their insightful comments and review of my thesis on a short notice. Last, but not least, I thank my wife Lilly for the support she gave me during my masters program. She has also been an inspiration throughout this journey.

Patrick Ochieng

BIOCHEMICAL CHARACTERIZATION OF DISEASE-CAUSING MUTATION IN N-TERMINAL WILSON PROTEIN DOMAIN SIX

Patrick Ochieng, M.S.
Western Michigan University, 2007

Wilson protein (ATP7B) is a copper-transporting P-type ATPase that regulates copper homeostasis and secretion of copper-containing enzymes in the liver. In hepatocytes, ATP7B delivers copper to apoceruloplasmin and mediates the excretion of excess copper into bile. Mutation in the gene coding for Wilson protein leads to Wilson disease. Several mutations in Wilson protein have been identified and of particular interest, mutations affecting the N-metal binding region significantly interfere with the ability of Wilson protein to transport copper to its target in the copper-trafficking pathway. In an attempt to characterize the disease-causing mutation (G591D) in Wilson protein domain 6 (WLN6), we have sub-cloned, overexpressed, purified and structurally characterized the native domain 6 construct of Wilson protein using NMR. We have also expressed the G591D mutant form of the same domain in GST fusion for comparison studies. Solution NMR results indicate that native WNL6 is monomeric and well-folded with a βαββαβ ferroxidin-like structure. Subsequent structural determination of this mutant with NMR will reveal more about the effect of this mutation.

TABLE OF CONTENTS

Table of Contents - Continued

CHAPTER

CHAPTER

CHAPTER

Table of Contents - Continued

CHAPTER

LIST OF TABLES

LIST OF FIGURES

List of Figures - Continued

LIST OF ABBREVIATIONS

WD .....Wilson Disease

MND.....Menkes Disease

WLNP.....Wilson Disease Protein

MNKP.....Menkes Disease Protein

MNK2.....Menkes Disease Protein N-terminal domain 2

MBD.....Metal Binding Domains

WLN6.....Wilson Protein N-terminal domain 6

WLN5-6.....Wilson Protein N-terminal domains 5 and 6

WD4.....Wilson Protein N-terminal domain 4

CD.....Circular Dichroism

IPTG.....Isopropyl β-D-1-thiogalactopyranoside

DTT.....Dithiothreitol

CHAPTER I

INTRODUCTION

Importance of copper and homeostasis

The association between the nutrient copper and normal hemoglobin metabolism, a vital physiological process, was recognized in the middle of the 19th century (Fox, 2003). Over the next 150 years, approximately a dozen proteins dependent on copper for their function (cuproenzymes) were discovered (Failla *et al.*, 2001). These cuproenzymes explain why dietary copper is essential, because copper restriction in the diet can alter the activity of a cuproenzyme and impact normal physiology. Copper plays a key role in all living organisms serving as a cofactor for many enzymes and proteins involved in electron transfer (cytochrome *c* oxidase), melanin production (tyrosinase), production of neurotransmitters (dopamine-β-hyroxylase), collagen cross-linking (lysyl oxidase) and detoxification of oxygen radicals (superoxide dismutase) (Yuan *et al.*, 1995). An example of the importance of copper is hereby outlined: In melanocytes the copper redox center of tyrosinase converts tyrosine to dihydroxyphenylalanine in the first step in the synthesis of the pigment melanin. Hypopigmentation is a consequence of dietary copper deficiency due to limiting tyrosinase. Other details of the nutritional biochemistry of copper have been summarized elsewhere (Prohaska, 1988). Excess copper inside the cells is also toxic. Some of the toxic effects of increased copper levels inside the cell include DNA damage, inactivation of certain enzymes and lipid peroxidation (Gu *et al.*, 2000). Excess copper(I) in the cells can also disproportionate to elemental copper whose interaction with hydrogen peroxide gives superoxide species which may lead to oxidative damage of cells (DiGuiseppi & Fridovich, 1984).

It is recommended that adults consume at least 0.9 mg of copper daily and restrict their intake to <10 mg daily to prevent overt signs of copper deficiency and toxicity, respectively (Trumbo *et al.*, 2001). Cells have therefore developed a tight-lipped homeostatic mechanism through which the uptake, distribution, secretion and the efflux of copper is mediated. The accomplishment of copper homeostasis and other toxic metals is still not yet fully understood and this represents a central problem in bioinorganic chemistry. The importance of understanding how metal ions are handled within cells is underscored by recent research linking a number of human diseases to deficiencies in metal ion trafficking pathways.

The molecular details of intracellular copper trafficking have been the centre of focus towards understanding the mechanisms of copper transfer and excretion. The discovery of copper handling proteins; copper chaperones (metallochaperones) and copper transporting ATPases has shed some light in copper regulation and transport. Proteins involved in the uptake, distribution, secretion and efflux of copper include high affinity permeases for copper uptake, copper chaperones for distribution to target copper requiring proteins and copper transporting P-type ATPases which transport copper in the secretory pathway and export copper when in excess (Huffman & O'Halloran, 2001; Prohaska & Gybina, 2004). The liver plays a very crucial role in copper balance in the body. Most copper absorbed from the intestine is received by the liver. Also biliary excretion is closely connected to the liver (Tao & Gitlin, 2003).

Intracellular copper pathways

Elevated copper levels inside the cell are harmful for the cell. Copper proteins in the body however, require threshold amounts of copper for either enhancement of their activities or for transport to its target in the copper transport pathway. Therefore a sequential mechanism through which this process is accomplished must be realized for the homeostatic balance to be attained. Copper acquisition, utilization and export is orchestrated by a series of copper permeases, copper chaperones and copper transporting ATPases (Huffman & O'Halloran, 2001).

In humans the Ctr1 permeases transports copper from the extracellular matrix into the cell (Kuo *et al.*, 2001). Before uptake inside the cell copper is first reduced from Cu^{+} to Cu^{2+} by a mechanism which is still not well understood (Lee *et al.*, 2002; Puig *et al.*, 2002). Once inside the cell, copper is acquired by the chaperones, CCS for superoxide dismutase (Casareno *et al.*, 1998) and Hah1 (also called Atox1) (Klomp *et al.*, 1997) for Wilson protein and/or Menkes protein. Figure 1 shows a schematic representation of how this transfer is accomplished. In humans, Atox1 delivers copper to the membrane associated copper-transporting ATPases. Wilson disease protein (WLNP) and Menkes disease protein (MNKP) ultimately use the energy derived from ATP hydrolysis to translocate copper into the secretory pathway and to export excess copper into the bile (Hung *et al.*, 1997). CCS delivers copper to Cu/Zn superoxide dismutase (SOD) while the chaperone that delivers copper to cytochrome *c* oxidase is still unknown. Recent studies indicate the possibility of mitochondrion matrix copper complex being the copper source for cytochrome *c* oxidase (Cobine *et al.*, 2006). Other putative copper handling proteins include Murr1 (a recently discovered protein whose absence results in canine copper

toxicosis) (Klomp *et al.*, 2003; Tao *et al.*, 2003), metallothionine (MT-1 and MT-2) and amyloid precursor protein (APP) (Kong *et al.*, 2007).

There has been remarkable conservation of the copper-binding sites in the metallochaperones and ATPases from bacteria to mammals (Arnesano *et al.*, 2002). For example, the sequence M-X^{I}-C-X^{II}-X^{III}-C is highly conserved. X^{I} is usually S, T, or H, and X^{III} is G in metallochaperones and S or A in ATPases. This suggests that these proteins are functionally related or belong to the same pathway. Analogous to the mechanism of copper trafficking in humans is the proposal that there is a similarity through which the yeast metallochaperone Atx1 delivers copper to its target Wilson protein homologue, Ccc2 (Pufahl *et al.*, 1997).

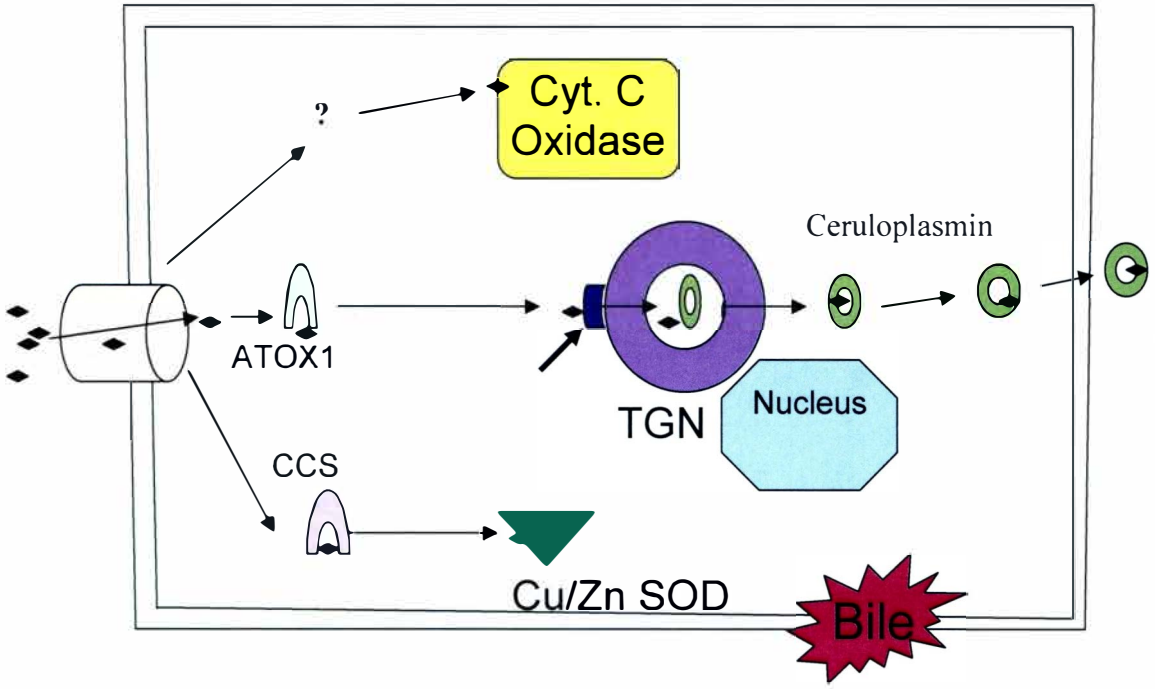

Figure 1. The copper trafficking pathways in hepatocyte. Cox 17, Atox1 and CCS are copper chaperones. Cytochrome *c* oxidase, Wilson/Menkes protein and Cu/Zn SOD are copper target proteins. TGN is *trans*-Golgi network.

Wilson Disease (WD)

Wilson disease, or hepatolenticular degeneration (Wilson, 1912), is a neurodegenerative disease of copper metabolism. Patients accumulate copper in the liver, kidneys and brain (Cumings, 1948). Later, more symptoms observed included renal dysfunction (Brewer & Yuzbasiyan-Gurkan, 1992), reduced copper incorporation in ceruloplasmin (Scheinberg & Gitlin, 1952) and impaired billiary excretion (Frommer, 1974; Sternlieb, 1984). Mutations in the ATPB7 proteins lead to disruption of normal copper distribution leading to Wilson Disease (Cox, 1996; Moore & Cox, 2002). Wilson disease involves loss of the ability to export copper from the liver into bile and to incorporate copper into hepatic ceruloplasmin. Accumulation of copper in the cytoplasm of hepatocytes results in cellular necrosis and leakage of copper into the plasma. The excess copper then collects in extrahepatic tissues, including the basal ganglia and the limbus of the cornea (Walter *et al.*, 2005).

Wilson disease incidence is 1 in 35,000-100,000 live births, with a gene frequency of 0.56% (Gollan & Gollan, 1998). The treatments that have been used to contain Wilson disease include agents such as BAL (2,3-dimercaptopropanol), D-penicillamine, zinc acetate, TRIEN (triethylenetetramine), and tetrathiolmolybdate. BAL, D-penicillamine, TRIEN, and tetrathiomolybdate are copper chelating agents which remove excess copper from the body. Zinc salts and tetrathiolmolybdate prevent the uptake of copper by the intestinal cells and increase fecal excretion (Brewer *et al.*, 2003).

Although the animal models are not human equivalents of Wilson disease, they are helpful in studying copper metabolism and potential treatments. The Bedlington terrier has an autosomal recessive inherited disease characterized by copper toxicosis (Klomp *et al.*, 2003). The Bedlington terrier does not develop neurological symptoms,

but its liver pathology is similar to that of Wilson disease. Canine copper toxicosis is caused by a mutation of the MURR1 gene, which is also believed to be essential for copper excretion and downstream of the gene that causes Wilson disease.

Menkes Disease (MKD)

The importance of copper homeostasis is underscored by Menkes and Wilson diseases (Culotta & Gitlin, 2001). In 1962, John Menkes, MD, and his colleagues at Columbia University in New York published a scientific article about 5 male infants with a distinctive genetic syndrome (Menkes *et al.*, 1962). This syndrome, now known as Menkes kinky hair disease, has been identified as a disorder of copper metabolism in the body. Some parts of the body don't have enough copper (blood plasma, liver, and brain), while other parts of the body (kidney, spleen, skeletal muscle) accumulate too much. Menkes disease is characterized by copper deficiency due to defective transport across the placenta and intestinal uptake of copper (Schaefer & Gitlin, 1999). Copper transport across blood the brain barrier is also impaired leading to severe copper deficiency in the central nervous system (Danks, 1995). Menkes disease is caused by mutations in the gene coding for the Menkes disease protein, MNKP. The major symptoms include neurological defects, weak muscles and poor growth which usually eventually leads to death (Schaefer & Gitlin, 1999). Menkes disease is estimated to occur anywhere from 1 individual per 100,000 live births to 1 in 250,000 live births (Danks, 1980). Logically, it would seem that if copper could get to the cells and organs that need it, the disorder would be lessened. Researchers have tried giving intramuscular injections of copper, with mixed results. It does seem that the earlier in the course of the disease that the injections are given, the more positive the results. Milder forms of the disease respond well, but the

severe form does not show much change. Intravenous administration of copper-histidine complex is being used as a preferred treatment (Christodoulou *et al.*, 1998).

Wilson Protein (WLNP)

Wilson disease protein (WLNP) is a copper-transporting P-type ATPase (Bull *et al.*, 1993; Tanzi *et al.*, 1993) that plays a key role in copper distribution in the liver, kidney and the brain (Lutsenko & Petris, 2003). Immunocytochemical studies have demonstrated that Wilson protein is localized in the *trans*-Golgi network (Hung *et al.*, 1997; Yang *et al.*, 1997) and exhibits a copper-dependent translocation to a cytoplasmic vesicular compartment (Guo *et al.*, 2005). Other studies have confirmed that the amino terminus of this protein binds copper (DiDonato *et al.*, 1997; Lutsenko *et al.*, 1997) and expression of the human Wilson protein in *ccc2*Δ yeast lacking the homologous ATPase (Iida *et al.*, 1998) and in the LEC rat, an animal model of WLNP (Wu *et al.*, 1994; Yamaguchi *et al.*, 1994), demonstrates restoration of cuproprotein synthesis, indicating a direct role for the Wilson protein in copper transport (Hung *et al.*, 1997; Terada *et al.*, 1998).

WLNP utilizes the energy of ATP hydrolysis to transport the metal into the secretory pathway for incorporation into copper-dependent enzymes such as ceruloplasmin (a multi-copper oxidase) and to export excess copper from the cell (Lutsenko & Petris, 2003). Upon elevated copper levels, Wilson protein translocates from its normal position in the *trans*-Golgi network to the *post*-Golgi cytoplasmic vesicular compartment, where it is responsible for biliary excretion of copper. (Hung *et al.*, 1997). Mutations in Wilson protein leads to the disruption of normal copper distribution, leading to a severe pathological disease in humans known as Wilson disease. Wilson disease

(WD) is an inherited disorder of copper metabolism characterized by hepatic cirrhosis and neuronal degeneration caused by a marked impairment in biliary copper excretion (Cox, 1996; Cuthbert, 1998). Another copper-transporting ATPase carrying out a similar function to Wilson protein is Menkes protein. Mutations in Menkes protein also lead to Menkes disease, a copper deficiency disorder. WLNP and other eukaryotic copper ATPases are unique among the P-type ATPases because they do not bind copper directly from the cytosol (where the amounts of free copper are low, (Rae *et al.*, 1999)), instead the copper is delivered to these ATPases by metallochaperones facilitated by protein-protein binding and subsequent exchange of copper to the metalloprotein (Banci & Bertini & Cantini & Felli *et al.*, 2006). Atox1 (Hah 1) serves as the metallochaperone for WLNP (Figure 1).

Wilson Protein has six N-terminal metal binding regions (domains, MBDs), each of which contains a conserved amino acid sequence GMXCXXC (where X can be any amino acid). The cysteine residues in the consensus sequence of each motif are responsible for copper binding during the copper transfer mechanism (Huffman & O'Halloran, 2001). Structure-based sequence alignments have also predicted the tertiary structure of these individual domains to exhibit a βαββαβ conformation (Arnesano *et al.*, 2002). Achila *et al.* have resolved the NMR solution structure of two of the six N-terminal metal binding domains 5 and 6 (WLN5-6) of Wilson protein (Achila *et al.*, 2006). The solution NMR structure of WLN5-6 supports the βαββαβ structure prediction of a *bis* ferrodoxin fold. NMR structures of several N-terminal domains of Menkes protein have been shown to exhibit the same conformation (Banci *et al.*, 2004; Banci & Bertini & Cantini & Chasapis *et al.*, 2005; Banci & Bertini & Cantini & Migliardi *et al.*, 2005; Banci & Bertini & Ciofi-Baffoni *et al.*, 2005; Banci & Bertini &

Cantini & DellaMalva *et al.*, 2006) suggesting that these proteins carry out similar functions. WLNP is composed of an N-terminal metal binding domains, eight transmembrane domains, an ATP binding domain (composed of 2 domains, the P domain and the N-domain) and the actuator domain based on similarity to the sarcoplasmic reticulum Ca^{2+} ATPase (Toyoshima *et al.*, 2000; Toyoshima & Nomura, 2002; Toyoshima & Mizutani, 2004).

Metal Binding Domains (MBDs) in WLNP and MNKP

Both Wilson and Menkes proteins have six metal binding domains in the N-terminus. The individual domains are about 72 amino acids long and share about 20-60% homology. This low similarity suggests that these domains may be functionally non-equivalent, especially with respect to interaction with the copper chaperone, Atox 1 (Achila *et al.*, 2006; Banci & Bertini & Cantini & Chasapis *et al.*, 2005). The solution NMR structure of Menkes protein domain 4 exhibits a compact ferrodoxin-like βαββαβ fold (Gitschier *et al.*, 1998) and the same fold is predicted for each of the individual metal binding domains of WLNP.

A copper binding site CXXC is housed in the highly conserved motif GMTCXXC which forms a loop within each of the metal binding sites. Conserved residues in all the metal binding sites are found in this loop thereby forming a suitable environment necessary for accepting copper from intracellular copper donors such as Atox1 (Wernimont *et al.*, 2004). Copper induced conformational analysis shows that both the secondary and the tertiary structural changes take place upon copper binding. These changes are thought to play both regulatory and functional roles (DiDonato *et al.*, 2000).

Function of the N-terminal Metal Binding Domains (MBD)

A number of studies have been carried out attempting to elucidate the function of the N-terminal metal binding domains. In heterologous assays in ccc2Δ yeast, mutations in the N-metal binding domains of WLNP and MNKP closest to the membrane portion of the enzyme hinder their ability to transport and incorporate copper into the yeast ceruloplasmin homologue, Fet3 (Forbes *et al.*, 1999; Iida *et al.*, 1998). The second and third metal binding sites could not substitute for the sixth MBD in loading copper into Fet3. Moreover, a study done using WLNP variants with mutations or truncations in the N-terminal domains found that copper stimulates catalytic activity cooperatively and that this requires the presence of MBDs 5 and 6 (Huster & Lutsenko, 2003). Metal binding domains 5 and 6 also seem to be the most critical for copper trafficking from the *trans*-Golgi to plasma membrane in higher eukaryotes (Cater *et al.*, 2004). All lower eukaryotes and some prokaryotes possess at least two MBDs close to the membrane portion of the copper pump (Arnesano *et al.*, 2002). The spatial separation of each of the WLNP metal binding domains within the N-terminus may help facilitate interactions between domains of WLNP. Each of these ~ 72 residue domains are connected to one another by a linker: 11 residues between WLN1 and WLN2, 42 residues between WLN2 and WLN3, 30 residues between WLN3 and WLN4, 57 residues between WLN4 and WLN5 and 8 residues between WLN5 and WLN6.

Transmembrane domains

The derived amino acid sequence of the Wilson's disease gene reveals the presence of motifs conserved in all members of the P-type family of cation transport proteins. The prototypes of this family include the Ca^{2+}-ATPase in the sarcoplasmic

reticulum, the Na^+/K^+-ATPase on the plasma membrane, and the H^+/K^+-ATPase in the cells lining the stomach. Each of these ATPases contains a consensus ATP-binding domain (GDGVND) and an aspartate residue (DKTGT) used to form the aspartyl phosphoryl intermediate essential for ion transport (Lutsenko & Petris, 2003; Pedersen & Carafoli, 1987).

Ca^{2+}-ATPase is composed of three major domains. The TM (transmembrane) domain consists of 10 TM segments and forms sites for binding and translocation of ions. It is linked to a cytosolic ATP-binding domain, which contains the catalytic site, and to an actuator domain, which plays an important role in conformational transitions of Ca^{2+}-ATPase. In turn, the ATP-binding domain was shown to consist of two structural units connected by a linker: the P-domain, which houses the DKTG motif (a site of catalytic phosphorylation) and the N-domain, which contributes to the binding of nucleotides (Toyoshima *et al.*, 2000). In contrast with Ca^{2+}-ATPase, very little is known about the structure and the mechanistic properties of WLNP. Although the membrane structure of the Wilson ATPase has not been experimentally determined, hydropathy plot analysis and site-directed mutagenesis suggests a protein with eight transmembrane domains where the amino and carboxyl terminus are located on the same side of the membrane (Bull & Cox, 1994). In addition to the consensus sequences noted above, the Wilson ATPase contains one additional region, a *CPC* sequence in the sixth transmembrane domain, which is conserved in all heavy metal membrane transporters (Lutsenko & Kaplan, 1995; Solioz & Vulpe, 1996). In the case of the Wilson ATPase, these three amino acids are essential for copper transport, implying a role for these cysteines in metal binding (Payne *et al.*, 1998; Schaefer & Gitlin, 1999). Other studies (Tsivkovskii *et al.*, 2002) demonstrated that WLNP undergoes catalytic phosphorylation at D1027 in the

DKTG motif, as expected for the P-type ATPases. Studies also found that the mutation H1069Q (the most frequent mutation in patients suffering from Wilson's disease) disrupts catalytic phosphorylation from ATP, suggesting that H1069 plays an important role in ATP binding (Tsivkovskii *et al.*, 2003). In fact, the most recent analysis of this frequent disease mutation, H1069Q, demonstrates that it does not significantly affect the structures of the N-domain, but prevents tight binding of ATP (Dmitriev *et al.*, 2006). Several other disease-causing mutations have been identified in the ATP-binding domain of WLNP. Whereas for some of them the effect on WLNP function can be predicted (*e.g.*, the mutation T1031I adjacent to the DKTG motif will probably disrupt catalytic phosphorylation), the specific consequences of other mutations are still unclear.

Phosphorylation of WLNP and MNKP

WLNP belongs to a large family of P-type ATPases. During their catalytic cycle, the P-type ATPases become transiently phosphorylated at the invariant aspartic acid residue in the sequence motif DKTG located in the ATP-BD (ATP-binding domain) of the protein (Lutsenko & Petris, 2003). The structural and functional properties of several members of this family, such as Ca^{2+}-ATPase of SR (sarcoplasmic reticulum) and plasma membrane Na^{+}, K^{+}-ATPase have been studied fairly extensively. For example, the high-resolution structure of SR Ca^{2+}-ATPase has been determined in two conformational states (the calcium-bound form, E1 (Toyoshima *et al.*, 2000), and the calcium-empty form in a complex with thapsigargin, E2 (Toyoshima & Nomura, 2002), providing the structural basis for understanding the mechanism of the ATP-driven ion transport. Similarly, a solution NMR structure of the N-domain of ATP7b has been resolved recently (Dmitriev

et al., 2006). The N-domain consists of a six-stranded β-sheet with two adjacent α-helical hairpins and, unexpectedly, shows higher similarity to the bacterial K^+-transporting ATPase KdpB than to the mammalian Ca^{2+}-ATPase or Na^+, K^+-ATPase. The common core structure of P-type ATPases is retained in the 3D fold of the N-domain; however, the nucleotide coordination environment of ATP7B within this fold is different. The residues H1069, G1099, G1101, I1102, G1149, and N1150 conserved in the P(1B)-ATPase subfamily have also been shown to contribute to ATP binding (Dmitriev *et al.*, 2006).

Besides its role as a cofactor, copper has been shown to regulate crucial post-transcriptional events such as protein phosphorylation. Copper modulates phosphorylation of its key transporter in humans WLNP (Vanderwerf *et al.*, 2001). Copper induced phosphorylation was observed to be fast and specific and correlates with the intracellular location of WLNP. Copper induced phosphorylation also requires the N-terminal domains (Vanderwerf *et al.*, 2001). It was proposed by the authors that WLNP phosphorylation could be among the molecular mechanisms by which copper regulates its own metabolism.

MNKP is transiently phosphorylated by ATP in a copper specific and dependent manner and appears to undergo conformational changes in accordance with classical P-type ATPase model (Voskoboinik *et al.*, 2001). The data obtained from this study also suggest that the catalytic cycle of MNKP protein begins with the binding of copper to the high affinity binding sites in the transmembrane channel followed by ATP binding and transient phosphorylation. Recent studies show that Cu^+ interacts with MNKP in a cooperative manner to regulate phosphorylation (Hung *et al.*, 2007).

Regulation of WLNP and MNKP

Even though copper uptake through Ctr1 is a critical step in the supply of copper to the liver cells, the continuous accumulation of copper in hepatocytes of WD patients suggests that copper homeostasis is not regulated at the uptake level (Gitlin, 2003). Atox1-mediated copper transfer activates WLNP (Walker *et al.*, 2002). Studies have shown that Atox1 can transfer copper to N-terminal WLNP as well as remove copper from the same region after incubation with apo-Atox1 (Walker *et al.*, 2002) and apparently down-regulation of WNDP activity. This suggests that both apo and metallated forms of Atox1 may contribute to the regulation of WLNP activity (Walker *et al.*, 2002).

Copper binding to N-terminal WLNP induces a metal-specific conformational change in WLNP protein (DiDonato *et al.*, 2000). Analysis of copper-induced conformational changes in the amino-terminal domain indicates that both secondary and tertiary structure changes take place upon copper binding (DiDonato *et al.*, 2000). These copper-induced conformational changes could play an important role in the function and regulation of the ATPase in vivo (Fatemi & Sarkar, 2002). This theory is also supported by experiments showing that copper occupancy of WLNP affects its intracellular localization, post-transcriptional modification and activity (Vanderwerf *et al.*, 2001).

Other studies using rCBD, an N-terminal rat homologue of WLNP, also show a metal induced secondary and tertiary structural changes similar to the one observed for WLNP (Tsay *et al.*, 2004). Analysis of the UV and CD spectra of rCBD suggests that Cu^{+} binding to N-terminal domains induces the conformational change. These observations support the theory of regulation by the copper substrate (DiDonato *et al.*, 2002).

Metal binding, coordination and metal ion specificity

Circular Dichroism (CD) and X-ray absorption Spectroscopy (XAS) have been used to characterize Zn binding to N terminal WLNP. Zn^{2+} is able to bind to this domain with a 6.5:1 stoichiometry (DiDonato *et al.*, 2002). Extended X-ray Absorption Fine Structure (EXAFS) experiments show that MBD2 (Walker *et al.*, 2004) and Atox1 (Ralle *et al.*, 2003; Ralle *et al.*, 2004) both bind Cu^{+} with a linear co-ordination and the distance between sulfurs in the cysteine residues to Cu^{+} is 2.16 Å in each protein. Electron Paramagnetic Resonance (EPR) analysis of copper bound MBD1 of MNKP showed no signal (Jensen & Bonander & Horn *et al.*, 1999). This confirms that copper-bound to MBD1 is in the +1 oxidation state and not +2. Cu^{+} was also observed to bind to apo MBD1 of MNKP in a 1:1 stoichiometry with an apparent K_d of 46 μM. However, oxidized MBD1 does not bind Cu^{+} (Jensen & Bonander & Horn *et al.*, 1999). Both N-WLNP and N-MNKP bind Cu^{+} with a stoichiometry of roughly 1:6 (DiDonato *et al.*, 1997; Jensen & Bonander & Moller *et al.*, 1999) suggesting that each of the six metal binding domains is involved in copper coordination. The apparent affinity constants for copper binding to WLNP N-terminal copper binding domains determined by isothermal titration calorimetry reveal similar values (K_a ~10^5-10^6) for all the domains (Wernimont *et al.*, 2004) which is on the same order as that measured for N-MNKP MBDs (Jensen & Bonander & Moller *et al.*, 1999).

Despite the high sequence similarity in P1-type ATPases, each ATPase is very discriminative in transporting its corresponding metal ions. For example ZntA, an *E. coli* P-type ATPase is specific for Pb^{2+}, Zn^{2+}, Cd^{2+} and Hg^{2+} while WLNP, MNKP and Cop A transport Cu^{+} and possibly Ag^{+} (Mitra & Sharma, 2001). A related study showed that

Zn^{2+} binds WLNP but is ligated to nitrogen atoms, not sulfur as for Cu^{+} (DiDonato *et al.*, 2002). This binding also induces conformational change on the protein. However, the conformational change is different and this may suggest a structure-based mechanism for discrimination of metal ions *in vivo*.

WLNP and MNKP have been found to be discriminative in the metal ion they bind and transport copper ions across the membrane. A study using immobilized metal ion chromatography reveals that the fusion protein of N-WLNP is able to bind transition metals with varied affinities as follows Cu^{+}>>Zn^{2+}> Ni^{2+}>Co^{2+}. N-WLNP shows no affinity for Ca^{2+}, Mg^{2+}, Fe^{2+}, and Fe^{3+} (DiDonato *et al.*, 1997).

Atx1-like copper chaperones

Metallochaperones are intracellular proteins that bind and deliver metal to specific partner proteins (Pufahl *et al.*, 1997). The oxygen toxicity of yeast mutants lacking Cu, Zn-superoxide dismutase (SOD) can be suppressed by the expression of a small antioxidant protein, Atx1, which was subsequently shown to be a copper chaperone (Lin & Culotta, 1995; Lin *et al.*, 1997). Shortly after the yeast work was published, a homolog in humans and other mammals, Atox1, was discovered (Klomp *et al.*, 1997). Human Atox1 contains 68 amino acids. Once Cu^{+} enters a cell, it binds to the copper-binding site of Atox1 and is transferred to its docking partners in the secretory pathway (Fig.1). Atox1 interacts with ATP7B in the hepatocyte and is thus required for proper biliary excretion of excess copper as well as delivery of copper for holoceruloplasmin (CP) synthesis. In yeast, two metallochaperone mediated copper delivery pathways have been characterized in detail (Figure 1). Atx1 is a 73 amino acid protein that binds Cu^{+} (Pufahl *et al.*, 1997) and delivers it to the P-type ATPase Ccc2 (Huffman & O'Halloran, 2000) for

translocation across intracellular membrane and loading into multicopper oxidase Fet3 (Yuan *et al.*, 1995). Fet3 is then localized to the cell surface where it is proposed to oxidize Fe^{2+} to Fe^{3+} for transport across the plasma membrane (de Silva *et al.*, 1997). Deletion of the gene encoding Atx1 in yeast cells results in defects in high affinity iron uptake (Lin *et al.*, 1997). Expression of the human Atx1 homologue Hah1 restores iron uptake in hah1Δ yeast, consistent with the presence of an analogous pathway in humans (Klomp *et al.*, 1997). In another experiment deletion of the Atox1 gene in mice causes perinatal mortality (Hamza *et al.*, 2001). Atox1-null mice exhibit hypopigmentation consistent with a role for Atox1 in copper delivery to tyrosinase (Prohaska, 1988). The skin distortion is likely due to reduced levels of lysyl oxidase, a cuproenzyme involved in elastic and collagen cross-linking. Copper levels in the liver and brain are decreased by 50% in mutants, consistent with an impaired efflux of copper from enterocytes (Hamza *et al.*, 2001). Cells lacking Atox1 have impaired movement of ATP7A in response to copper, providing a mechanistic explanation for copper retention (Gitlin, 2003). ATP7A normally resides in the *trans*-Golgi membrane but moves to the plasma membrane when cellular copper concentrations rise (Monty *et al.*, 2005). In addition to its chaperone function, other properties may be ascribed to Atox1. Atox1 is present at high levels in neurons and may protect these cells from oxidative stress (Klomp *et al.*, 1997).

The copper-trafficking pathway in yeast has been extensively studied and much has been proposed. The reactivity of aqueous Cu^{+} and relative stability of Cu^{+} in Cu^{+}-Atx1 suggests that the coordination environment of Atx1 stabilizes the Cu^{+} state, suppressing the disproportionation of Cu^{+} to Cu^{2+} (aqueous) and Cu (Pufahl *et al.*, 1997). A direct, copper-dependent interaction between Atx1 and the first N-terminal domain of Ccc2 (Ccc2a) has been shown (Huffman & O'Halloran, 2000; Pufahl *et al.*, 1997).

Using this knowledge and the coordination chemistry of Cu^{+}-Atx1, a mechanism for copper exchange between Atx1 and Ccc2a has been proposed. The authors suggest that Cu^{+} is transferred from one protein to another through two- and three-coordinate intermediates.

An *in vitro* metal transfer assay has been developed to study the copper-trafficking pathway in yeast. Cu^{+}-Atx1 was mixed with apo-Ccc2a and separated using anion exchange chromatography. Using this assay, it was found that copper rapidly equilibrates between Atx1 and Ccc2a with an equilibrium constant of exchange ($K_{exchange}$) slightly > 1 (Huffman & O'Halloran, 2000). The transfer occurs in the presence of copper chelators, supporting the hypothesis that the copper exchange occurs through direct protein-protein interaction. Experiments repeated with Hg-Atx1 established that Hg-Atx1 is able to function as a model for the Cu^{+} form of Atx1 (Cu-Atx1) (Rosenzweig *et al.*, 1999).

Hah1, a human homologue of Atx1, has been shown to interact with Wilson Protein, a human homologue of Ccc2. Hah1 is localized to the cytoplasm and nucleus, and its interaction with WLNP is specific and copper-dependent (Hamza *et al.*, 1999). This interaction is impaired in WLNP with mutations that result in Wilson disease. In a GST column-binding assay, a smaller amount of the Wilson protein disease-causing mutants was retained on a GST-Hah1 column than the wild-type WLNP suggesting that there is poor interaction between mutant WLNP and its metallochaperone, Hah1 (Hamza *et al.*, 1999). A yeast two-hybrid system has been used to study the interaction and transfer of copper from Atox1 to various N-terminal domains of WLPN (Larin *et al.*, 1999). The metal-specific interaction between Atox1 and WLNP requires cysteine residues. The copper-transporting ability of Atox1 has also been shown to protect

neuronal cells from high copper concentration (Kelner *et al.*, 2000). This suggests that Atox1 could be involved in copper regulation in the body.

The homology between the human and yeast copper-trafficking systems have resulted in extending studies of the yeast system to the human system. There is new evidence for direct protein-protein interaction (Banci & Bertini & Cantini & Felli *et al.*, 2006), showing how the proteins interact and the molecular factors that define the proteins specificity. The determination of a high-resolution 1.02 Å X-ray structure of Hg-Atx1 has contributed to the understanding of the surface characteristics important for interaction (Rosenzweig *et al.*, 1999). The βαββαβ secondary structural domain of Atx1 places it in a structural class with the domain four of the MNKP (Gitschier *et al.*, 1998). The structural homology between Menkes 4 and Atx1, suggesting that Ccc2a and Ccc2b may also have a structure similar to Atx1, was shown in the NMR structure of Ccc2a (Banci *et al.*, 2001).

The crystal structure of Hg-Atx1 (Rosenzweig *et al.*, 1999) and its relationship to other copper-transporting proteins provides information about the residues important for protein interaction and metal transfer. There are 10 lysine residues on the surface of Atx1. Menkes protein domain 4 has multiple negatively charged residues (aspartate and glutamate) on the surface. It was hypothesized that some of these residues of Atx1 could interact with acidic residues on the surface of Ccc2 (Rosenzweig *et al.*, 1999). In support of this hypothesis, it has been demonstrated that the lysine residues on the surface of Atx1 are critical for the delivery of copper from Atx1 to Ccc2 (Portnoy *et al.*, 1999).

Copper Chaperone, CCS

The second copper chaperone to be recognized, CCS, is a protein required for the delivery of copper to SOD under copper limiting conditions. This chaperone was discovered by Valerie Culotta and colleagues (Culotta *et al.*, 1997). CCS is a homodimer with 35-kDa subunits and 3 functional domains. Domain 2 is highly homologous to SOD. Heterodimer pairs of SOD and CCS subunits form to facilitate copper transfer (Rae *et al.*, 1999; Schmidt *et al.*, 1999). Domain 1 contains the MXCXXC copper-binding site but essential cysteines in domain 3 are involved in the transfer of copper to apoprotein (apo)-SOD.

CCS deletion greatly reduces SOD activity in mice (Wong *et al.*, 2000). The phenotype of CCS –/– mice is similar to that of SOD1 –/– mice with increased sensitivity to oxidant challenge. Lack of CCS does not alter other copper chaperone–dependent pathways, such as ceruloplasmin activation (Wong *et al.*, 2000). A fraction of yeast CCS is located in the mitochondrial intermembrane space with SOD (Sturtz *et al.*, 2001). Prohaska *et al* detected both CCS and SOD in purified rat brain mitochondria (Prohaska & Gybina, 2004). Presumably, SOD in the mitochondria can scavenge superoxide released toward the intermembrane space, whereas matrix-generated superoxide can be disposed of by manganese-dependent superoxide dismutase (SOD2). In yeast, CCS is necessary for copper transfer to apo-SOD under copper-limiting conditions, because the free ionic copper content is extremely low (Rae *et al*, 1999). Work with CCS –/– mice indicate a similar dependence on CCS in mammals (Wong *et al.*, 2000).

A number of groups have independently reported elevated CCS levels in tissues of copper-deficient mice and rats (Bertinato *et al.*, 2003; Prohaska *et al.*, 2003). This effect

was not due to enhanced synthesis of CCS, as evidenced by unchanged mRNA levels in both rats and mice. Cell culture studies indicate that elevated CCS levels in copper-limited cells is due to slower degradation by the 26S proteosome complex (Bertinato & L'Abbe, 2003). CCS levels are not correlated with SOD levels in mammals. Higher brain CCS levels in mice and rats have been observed even though SOD levels were unchanged (Prohaska *et al.*, 2003). In some tissues, such as the liver, SOD protein levels are markedly lower following copper deficiency or deletion of CCS protein (Prohaska *et al.*, 2003). Cell CCS levels are affected by copper status. In fact, elevated CCS concentration is one of the most robust cuproprotein changes following copper deprivation. Changes in CCS concentration may be a useful way to assess copper status in humans.

Other potential copper handling and/or sensing proteins

Other copper sensing proteins have recently been discovered. Murr1 directly interacts with ATP7B (Tao *et al.*, 2003). The loss of Murr1 causes hepatic copper overload. Murr1 does not directly interact with Atox1, suggesting that Murr1 may be required for the movement of copper to the bile from ATP7B.

Metallothionine (MT) is a low-molecular-weight cysteine-rich protein whose function remains elusive (Coyle *et al.*, 2002). Two isoforms of MT, MT-1 and MT-2, may play a role in intracellular copper transfer and storage. In the perinatal liver, copper stores are associated with MT, perhaps because of an immature biliary secretory system and limited ceruloplasmin synthesis. Copper can induce MT synthesis, although zinc is more likely the physiological inducer (Coyle *et al.*, 2002). It has been suggested that MT

plays an important role under these conditions as well, by acting as a copper reserve (Suzuki *et al.*, 2002).

APP (amyloid precursor protein) is a membrane protein that contains a copper-binding site. In APP-null mice, brain copper levels are markedly elevated, compared to those in wild-type mice (White *et al.*, 1999). Brain zinc and iron levels are unaffected. Conversely, in transgenic mice that overexpress APP, brain copper levels are reduced (Maynard *et al.*, 2002). This suggests that APP serves as a barrier to copper import in the brain. Dietary copper supplementation can reverse both the reduction in brain copper levels and lower the SOD activity observed in APP overexpressors (Bayer *et al.*, 2003).

Structures of WLNP and MNKP

Both WDP and MNK have eight putative transmembrane domains, and the sixth bears a CPC (Cysteine-Proline-Cysteine) motif which is also thought to bind to metal ions (Lutsenko & Petris, 2003). Besides, there are six soluble N-terminal metal binding domains each containing a conserved CXXC metal binding motif (Figure 2) (Bull & Cox, 1994). The gene that encodes WLNP is localized on chromosome 13 at loci q14.3 (Frydman *et al.*, 1985). WLNP is 1465 amino acids long and therefore has a molecular weight of 159 kD.

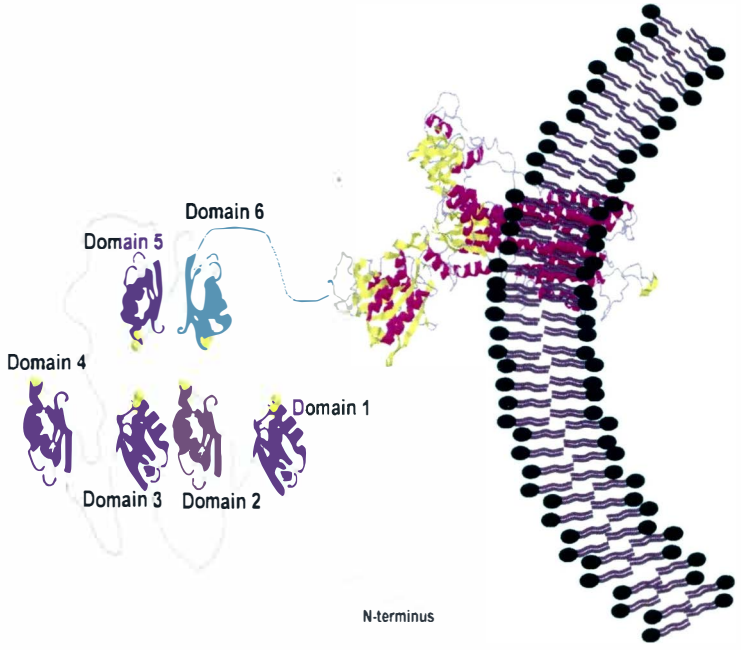

Figure 2. Model of Wilson Disease Protein. Domains 1-6: N-terminal metal binding domains. Yellow and purple ribbons are the transmembrane domains.

X-ray crystallography and NMR spectroscopy have provided structures of various metal-binding domains in different metallation states for both metallochaperones and the partner ATPases (Achila *et al.*, 2006; Banci *et al.*, 2001; Banci *et al.*, 2004; Banci & Bertini & Cantini & Chasapis *et al.*, 2005; Banci & Bertini & Cantini & Migliardi *et al.*, 2005; Banci & Bertini & Ciofi-Baffoni *et al.*, 2005; Banci & Bertini & Cantini & DellaMalva *et al.*, 2006; Banci & Bertini & Cantini & Felli *et al.*, 2006; Gitschier *et al.*, 1998; Rosenzweig, 2001). In some cases, the dynamic properties of the apo- and/or holoproteins have been directly probed by NMR in solution (Achila *et al.*, 2006; Banci *et al.*, 2001; Banci *et al.*, 2004; Banci & Bertini & Cantini & Felli *et al.*, 2006; Dmitriev *et al.*, 2006).

Recently, Achila *et al*, have elucidated the apo-structure of multi-domain construct of domains 5 and 6 together using NMR (Achila *et al.*, 2006) (Figure 3). The tertiary structure of these two individual domains are shown to assume a βαββαβ conformation.

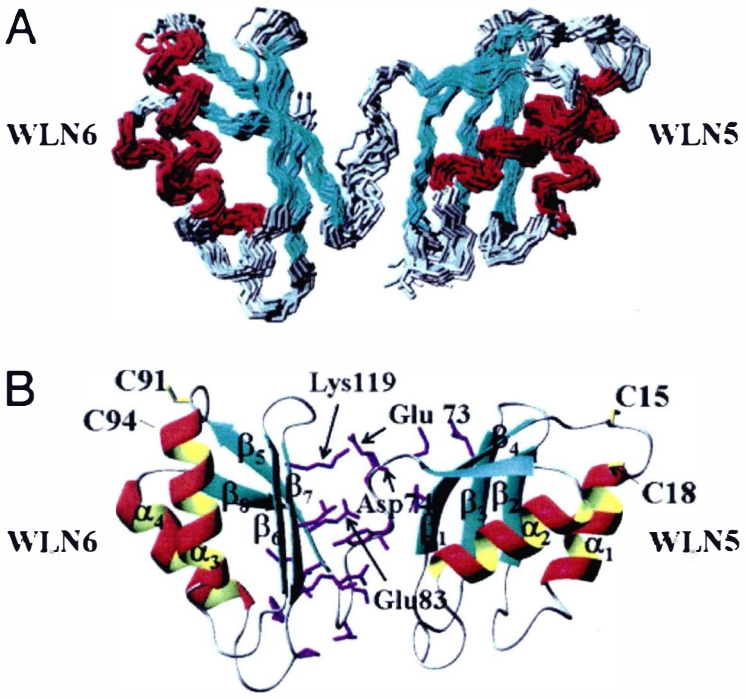

Figure 3: Solution structure (ribbon representation) of apoWLN5–6. (The secondary structure elements are indicated: β-strands are cyan and α-helices are red (Achila *et al.*, 2006).

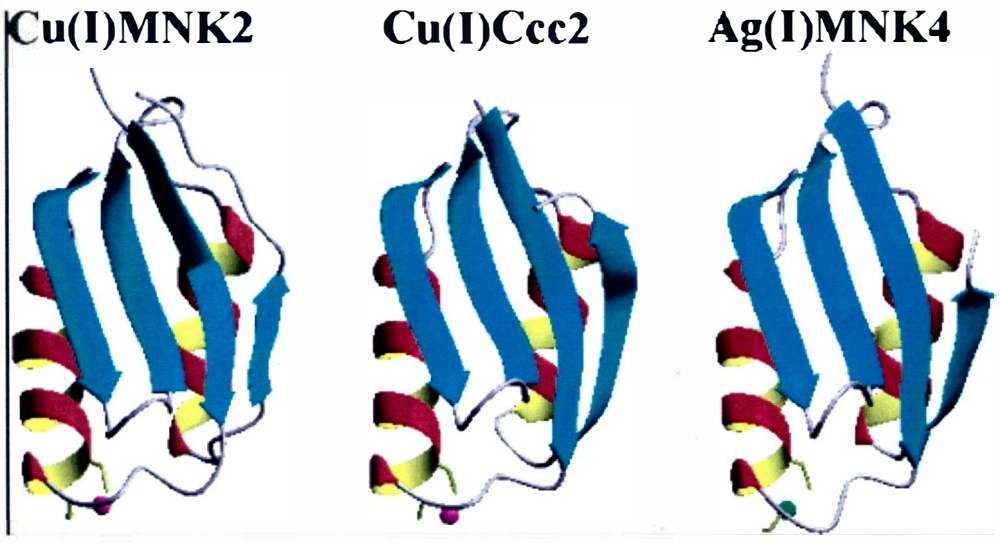

Figure 4: Ribbon representations of the structures of (from left to right) copper(I)-bound MNK2, copper(I)-bound Ccc2 and silver(I)-bound MNK4. The side chains of the metal-binding cysteins are shown in yellow; the metal ions are shown as pink copper(I) or green silver(I) (Banci *et al.*, 2004).

The yeast homologue of Wilson protein, Ccc2, contains two N-terminal binding domains each bearing the conserved CXXC metal binding motif (Yuan *et al.*, 1995). It is also important to note that the structure of each domain of Ccc2 assumes a βαββαβ conformation (Figure 4). Human copper chaperone, Atox1. and its homologues found in both eukaryotes and prokaryotes contain a single CXXC motif (Rosenzweig, 2001).

Interaction of Atox1 with Wilson Protein

Human copper chaperone, Atox1, plays a key role in copper distribution to the secretory pathway of the cell. Insights regarding the interaction of this metallochaperone and its target protein, WLNP, have been realized from studies carried out in yeast. Atox1 is an ortholog of yeast Atx1 which is responsible for transporting copper into the Golgi

compartment (Pufahl *et al.*, 1997). This observation is supported by an experiment in which Atx1 gene is deleted in mice leading to copper accumulation and decreased activity of secreted copper dependent enzymes such as tyrosinase (Hamza *et al.*, 2001). Several studies have shown evidence for physical interaction between Atox1 and WLNP or MNKP (Achila *et al.*, 2006; Hamza *et al.*, 1999; Larin *et al.*, 1999; van Dongen *et al.*, 2004). In a study utilizing a glutathione S - transferease-Atx1 fusion, there was direct protein - protein interaction between Atox1 and WD1-4 and that the interaction depended on the presence of the copper ligands, CXXC in the N-terminus of Atox1 (Hamza *et al.*, 1999). This finding was supported by co-immunoprecipitation experiment which also revealed that Atox1 interacts both with Wilson protein and Menkes protein in a copper dependent fashion (Hamza *et al.*, 1999). A similar study to test disease-associated mutations in the N-terminal WLNP showed a decrease in Atox1 interaction with mutated WLNP proteins (Hamza *et al.*, 1999). Impaired copper delivery by Atox1 is proposed to constitute the molecular basis of Wilson disease in patients harboring these mutations (Hamza *et al.*, 1999).

A systemic yeast two hybrid screening of interaction between copper binding domains showed that Atox1 interacts with MBDs 2 and 4 of WLNP. MBD4 of WLNP showed the strongest interaction with Atox1 (van Dongen *et al.*, 2004) suggesting that these domains may be responsible for copper uptake from the metallochaperone before distributing copper to the other domains. NMR studies carried our by Achila *et al*, also indicates that there is complex formation between Atox1 and Wilson protein domain 4 (Achila *et al.*, 2006). The relaxation measurement values indicate that there is a fast exchange of the complex with the free proteins in solution. The equilibrium of this reaction also appears to be similar to that experienced by Ccc2a and Atx1 (Arnesano *et*

al., 2001; Banci & Bertini & Cantini & Felli *et al.*, 2006), a metal-mediated protein-protein interation. All the interactions between Atox1 and single domains are found to be weaker compared to the multidomain construct WLNP 1-4 (Larin *et al.*, 1999).

It is logical that for the subsequent transfer of copper to take place from one protein to another, there is a need for protein-protein interaction. Walker *et al.* observed that copper transfer from Atox1 to the N-terminal WLNP results in selective shielding of cysteines in domain 2 against labeling with a cysteine-directed probe, an observation that is absent when free copper (without Atox1) is added (Walker *et al.*, 2004). They also found that mutagenesis of WLNP domain 2 knocks out the stimulation of catalytic activity of WLNP by the Cu-Atox1 complex but not by free copper. Based on these observations, the authors (Walker *et al.*, 2004) suggested that Atox1 specifically delivers copper to domain 2 alone, at odds with protein-protein interaction experiments showing a stronger interaction with domain 4 (Achila *et al.*, 2006; van Dongen *et al.*, 2004).

The authors (Walker *et al.*, 2004) therefore proposed that the preference of Atox1 for domain 2 may not be due to higher copper binding affinity for domain 2 nor appropriate exposure of the metal coordinating residues but due to specific protein-protein interactions. They state that this specific interaction is enabled by the complementation of negatively charged patch at the surface of domain 2 and positively charged patch on Atox1. The authors (Walker *et al.*, 2004) observed that copper bound to WLNP domain 2 did not migrate to other metal binding domains; therefore, this could support a proposal that WLPN domain 2 works as a switch allowing subsequent loading of other sites. The initial entry site of copper from the Atox1 metallochaperone still remains unresolved, but future experiments should compare copper delivery from Atx1 to other domains in the full length WLN1-6 construct. Recent studies from the Rosenzweig

laboratory showed copper transfer to each of the domains from Cu-loaded Atox1 in a full-length six domain construct (Yatsunyk & Rosenzweig, 2007).

Mutations in Wilson Protein

A number of mutations (over 100) in the Wilson protein gene have been identified (http://www.medicalgenetics.med.ualberta.ca/wilson/index.php) and of particular interest, mutations affecting the N-metal binding region significantly interfere with the ability of Wilson protein to transport copper. Mutations in the N-terminal region include G85V in domain 1, L492S in domain 5, Y532H in domain 5, and G591D in domain 6 (Cox *et al.*, 2005; Loudianos *et al.*, 1998). Several studies have shown that domain 6 of Wilson protein is more essential for proper function of Wilson protein. Iida *et al.* have shown the importance of domain 6 by introducing domain six (*i.e.*, WLNP lacking domains 1-5) to yeast lacking Ccc2, a Wilson protein homologue (Iida *et al.*, 1998). Human Wilson protein with domain 6 but lacking other domains rescued the dying yeast. These results indicate that all the six domains are not functionally equivalent and that WLN6 is important for proper functioning of Wilson protein. Furthermore, Forbes *et al* have also emphasized the importance of domain 6 by mutating or deleting domains 1 through 5. Their findings show that this deletion or mutation does not significantly interfere with the function of Wilson protein and that domain 6 alone is sufficient in yeast complementation assays (Forbes *et al.*, 1999). Also, it has been shown that there is impaired interaction between Atox1 (the copper chaperone responsible for delivering copper to Wilson protein) and Wilson protein containing the G591D mutation in domain 6 (Hamza *et al.*, 1999). Since copper transfer only occurs with concomitant metallochaperone-ATPase interaction, copper delivery is thus hindered.

There is no doubt therefore that Wilson protein domain 6 plays a significant role in the proper functioning of this protein. To date there is no molecular study that has been carried out in any of the Wilson protein disease-causing mutations and this study therefore focuses on unraveling the molecular impairment of the mutant protein (G591D) in metal binding domain 6. The results obtained could be used to understand the important role that the MBDs play in the copper transport process. Therefore we are expressing both the wild type and mutant (G591D) forms of this protein and subsequently characterize this disease-causing mutation. Banci *et al.* have investigated the disease-causing mutation A629P in the sixth metal binding domain of WLNP protein homologue, Menkes protein (Banci & Bertini & Cantini & Migliardi *et al.*, 2005). Their investigation reveals that the Menkes A629P mutation makes the protein β sheet more solvent accessible and possibly resulting in an enhanced susceptibility of ATP7A to proteolytic cleavage and/or reduced capability of Cu^{+} translocation. Similar behavior may also be observed with Wilson disease protein mutant G591D. Mutation experiments and molecular characterization techniques must therefore be carried out in both native and mutant forms to understand this mutation.

Objectives of this study

In this research, we have sub-cloned, expressed and purified the wild type form of Wilson protein domain 6 construct for our studies, alongside the mutant form (G591D). The other objectives of this study were to elucidate the solution NMR structure of native and mutant WLN6. The ultimate goal of this research is to structurally characterize the disease-causing mutation in domain 6 of Wilson protein. This will allow us to understand

the effects of this mutation and subsequently the copper transport mechanism inside the cell. Also we have expressed WLN4 and WLN2 with the ^{13}C and ^{15}N isotopic labels. This will allow us elucidate their NMR structure as well.

CHAPTER II

EXPERIMENTAL METHODS

Materials

The ATP7B gene was obtained as a donation from Dr. Jonathan Gitlin of the University of Washington, St Louis Missouri. All the primers were purchased from Integrated DNA Technologies, Inc. Restriction endonucleases, relevant enzymes and buffers were purchased from New England Biolabs Inc and Life Technologies. Nucleotides and citric acid were purchased from Sigma Chemicals Company. Bacterial strains and plasmids were purchased from Novagen while the QIAGEN Plasmid and DNA Isolation Kits were purchased from QIAGEN Inc. Dimethyl sulfoxide (DMSO), monobasic and dibasic potassium phosphates were purchased from J.T Baker Chemical Company. Isopropyl -β-D-thiogalactopyranoside (IPTG) was purchased from INALCO SPA (Italy).

Sodium phosphate (monobasic and dibasic), sodium chloride, yeast extract, dextrose and 2-(4-morpholino)-ethane sulphonic acid (MES) were purchased from Fisher Chemicals. Deuterium oxide was purchased from Aldrich Chemicals. Coomasie plus dye was purchased from Pierce while Bio-Rad Dye for Bradford Assay was purchased from Bio-Rad Laboratories Inc. Bacto-Agar for making Agar plates was purchased from DIFCO while Agarose from Gibco BRL. Kanamycin sulfate was purchased from Calbiochem. YM3 membranes and Centricons for protein concentration were obtained from Amicon Bioseperations, NMR tubes were purchased from WILMAD LabGlass.

Cloning of WLN6 gene into pET 24d

Before cloning of WLN6 into the pET 24d plasmid vector, the human cDNA Wilson protein gene was obtained as a donation from Dr. Jonathan Gitlin of Washington University, St. Louis. Both forward and reverse primers for domain 6 amplification were designed as described below.

Primer design

The primers were designed with the DNA Strider program. The sequence for the forward primer was: 5'-GGA GGA CTA CGC ATC CAT GGA TGG CAA CAT TGA GCT GAC-3'. This primer design included a start codon ATG which codes for methionine and an NcoI restriction site CCATGG. The sequence of the reverse primer was 5-GAG CGT TGG GAT CCT ACT GGG CCA GGG-3'. This design incorporated a stop codon ACT and a unique restriction site for BamHI, GGATCC.

WLN6 amplification

The gene encoding WLN6 was amplified using the Polymerase Chain Reaction (PCR) utilizing the designed primers. Taking into account the Guanine-Cytosine (GC) content and the melting temperatures of the respective primers, the following written programme was used to facilitate the polymerization activity.

-Melting temperature 95°C for 5 min.

-Annealing Temperature 65°C for 1 min.

-Extension temperature 72°C for 40 sec.

-Melting at 95°C for 40 sec.

-Annealing at 65°C for 1 min.

-Extension at 72°C for 1 min.

Steps 4-6 were repeated 30 times. This was followed by storage in 4°C. Annealing temperature (T_m) was calculated from the composition of the primer according to Wallace rule (Equation).

$$[T_m\ (\text{In}\ ^{o}C) = (G + C) \times 4 + (A + T) \times 2] \qquad 2.1$$

The PCR product obtained was visualized in an agarose gel electrophoresis before purification. The product was subjected to purification using QIAquick Spin PCR purification kit. Purified DNA was analyzed using 1% Agarose gel electrophoresis. The gel was stained in ethidium bromide and visualized under UV light. The correct mass of the DNA was observed.

Cloning of WLN6

pET24d Novagen expression vector was digested using restriction enzymes NcoI and BamHI. Purified WLN6 gene was then ligated to pET24d vector using ligase enzyme (ligation product was named pPOWD6) at 16 °C for 10 hrs. The success of ligation was confirmed by DNA sequencing in the laboratory of Dr. Todd Barkman at Western Michigan University. Restriction analysis was also done to confirm ligation.

Transformation of pPOWD6 recombinant plasmid into DH5α cells

Competent DH5α cells (200 μL each) were thawed in ice before addition of 3 μL of dimethylsulfoxide (DMSO). 20 ng of undigested pET24d was added into the positive control tube, a similar mass of pPOWD6 recombinant plasmid added to another tube and 2 μL of milliQ water added to the negative control tube. These three tubes were placed on

ice for 15 minutes. The cells were then heat-shocked at 42°C for 2 min. and then set on ice for another 2 min. 1 mL of LB was finally added to each tube. These tubes were incubated at 37°C with subsequent shaking at 250 rpm for 1 hr. After 1 hr, the tubes were centrifuged and the pellet was resuspended in 200 μL of LB. The cells were plated on 3 different LB plates containing 30 μL/mL kanamycin. After 10 min, the plates were incubated at 37°C for 16 hr.

Inoculation of transformed colonies

Randomly selected colonies were inoculated in 3 culture tubes containing 5 mL LB containing 30 μL/mL kanamycin. The cultures were incubated at 37°C with shaking. The growth of the cells was monitored by periodically measuring the optical density (OD_{600}). When the OD_{600} reached 1, the culture was centrifuged and the pellet recovered. Plasmid DNA was recovered using the Qiagen mini plasmid kit.

Analysis of recovered plasmid

The purified plasmid recovered from the above transformation was analyzed using agarose gel electrophoresis. The plasmid was also subjected to restriction analysis and DNA sequencing. Restriction analysis was performed by digesting the recombinant plasmid with BamHI and NcoI. Successful clones were corresponded to the size of the insert based on the number of base pairs. The recombinant plasmid was also sequenced in Dr Barkman's Laboratory of Western Michigan University, Department of Biological Sciences.

Transformation of recombinant DNA (pPOWD6) in Rosetta cells

Two aliquots of *E. coli* Rosetta (DE3) strain cells (200 μL each) were thawed (Control and investigative) in ice before addition of 3 μL of dimethylsulfoxide (DMSO). 20 ng of recombinant DNA (pPOWD6) was added into the positive control tube, a similar mass of pPOWD6 recombinant plasmid added to another tube and 2 μL of water added to the negative control tube. These three tubes were placed on ice for 15 min. The cells were then heat-shocked at 42°C for 2 min. and then placed on ice for another 2 min. 1 mL of LB was finally added to each tube. These tubes were incubated at 37°C with subsequent shaking at 250 rpm for 1 hr. After 1 hr, the cells were centrifuged down using a microcentrifuge and resuspended in 200 μL of LB. The cells were plated on 2 different LB plates containing 30 μL/mL kanamycin. After 10 min., the plates were incubated at 37°C for 16 hr.

Test induction of WLN6 protein

Some colonies observed from the previous transformation of WLN6 with Rosetta cells were screened for protein induction. This test set up was done to analyze the induction levels of WLN6 protein. A single colony from the LB plate under investigation was inoculated in 5 mL LB treated with kanamycin sulfate (30 μg/mL). The inoculated culture was then incubated in a shaker set at 37°C with continuous shaking at 250 rpm until attainment of OD_{600} of approximately 0.6.

The culture was then pelleted by centrifugation and subsequently resuspended in 50 mL of LB medium treated with 30 μg/mL kanamycin. This culture was also incubated in the shaker as described earlier. The OD_{600} was periodically monitored using UV-Vis spectrophotometer. When the OD_{600} reached 0.6, Isopropyl-β-thiogalactopyranoside

(IPTG) was added to an effective concentration of 1 mM. The change in OD_{600} was monitored every 30 min. with successive withdrawal of 0.5 mL sample at every measurement. Induction was continued for 4 hr. The aliquots withdrawn from each 30 min. time interval were pelleted and prepared for SDS-PAGE.

The pelleted samples were prepared for SDS-PAGE as follows: the pellets were treated with 5 μL of loading buffer and 20 μL of water then heated to 92°C for 5 minutes. A 15% SDS-polyacrylamide gel was prepared. The induction samples were loaded in the wells of the gel. The gel was then run at 72 mV for 1 hr, stained with coomassie blue dye for 6hr and then destained for a similar time. Gel drying was finally performed using a mini gel drying unit from Invitrogen.

Production of WLN6 protein

With a positive induction from WLN6 protein test induction, a 10 L induction was carried out starting with inoculating 5 mL of LB with a fresh, single colony transformed in Rosetta cells. This culture was subjected to shaking at 37°C, the OD_{600} was also monitored. After the OD_{600} reached 0.6, the culture was transferred to another 100 mL LB treated with 30 μg/mL kanamycin for further growth. This was now used as the starter culture of the 10 L protein production. The 10 L LB treated with 30 μg/mL kanamycin was set in the fermentation tank and inoculated for growth. (Microferm fermenter, New Brunswick Scientific Co.). When the OD_{600} reached 0.6, protein expression was induced with 1 mM IPTG. After 4 hr, the cells were harvested by centrifugation at 6000 rpm for 20 min. in a SLA 3000 rotor. The pellet was stored at -20°C overnight before protein extraction.

WLN6 protein extraction and purification

Freeze/thaw extraction

The *E. coli* cells with overexpressed WLN6 were frozen for 5 min. with liquid nitrogen then allowed to thaw at room temperature successively for 3 cycles. The pellet was then resuspended in 240 mL (24 mL per liter of culture) extraction buffer (20 mM MES/Na, 1 mM EDTA, 10 mM Dithiothreitol (DTT), pH 6). The suspension was agitated in ice for 1 hr. Non-soluble portions of the cells were pelleted by centrifugation at 6000g for 15 min. at 4°C. The protein containing supernatant was decanted from the pellet and filtered through a 0.22 μM filter in preparation for anion-exchange chromatography. Pre and post-filtration samples were taken for later Bio-Rad analysis. WLN6 protein was purified in two chromatographic steps: anion exchange chromatography (DEAE column) and gel filtration.

Anion exchange chromatography

An Amersham Pharmacia Biotech DEAE sepharose fast-flow chromatographic column (Pharmacia, 2.6 cm x 13 cm, 69 mL) was packed with DEAE Sepharose resin to yield a total volume of approximately 70 mL). The column was then equilibrated with buffer A (20 mM MES/Na, 1 mM EDTA, 10 mM DTT, pH 6). The filtered supernatant from the freeze-thaw extraction step was then loaded onto the column. The first 50 mL of eluent from the column was collected and named 'flowthrough 1' while the next 190 mL was collected and named 'flowthrough 2'. The unbound protein was eluted from the column using 2 column volumes wash of Buffer A and this was collected and named 'column wash'. The protein bound onto the column was eluted using a salt gradient over

3 column volumes. A program was designed to elute the proteins with a mixture of buffer A (20 mM MES/Na, 1 mM EDTA, 10 mM DTT, pH 6) and Buffer B (20 mM MES/Na, 1 mM EDTA, 1 M NaCl, 10 mM EDTA, pH 6) at an increasing salt gradient until a maximum salt concentration of 50%. The eluent was collected in 95 fractions of 2.5 mL each. The Bio-Rad protein assay was performed for every fraction. The fractions containing WLN6 protein were confirmed by 15% SDS-PAGE. The fractions containing WLN6 protein were combined and concentrated down to 2 mL with an Amicon device using a YM3 membrane and pressurized nitrogen.

Gel filtration chromatography

WLN6 protein was separated from higher molecular weight impurities with size exclusion chromatography (gel filtration). First, a pre-packed Amersham Pharmacia Superdex-75 26/60 gel filtration column was washed with one column volume of filtered water at a flow rate of 2.6 mL/min. The column was then equilibrated with two column volumes of buffer (20 mM MES/Na, 150 mM NaCl, 10 mM DTT, pH 6). The concentrated protein solution containing WLN6 protein was loaded into the injection loop. A large superdex gel filtration computer programme was activated to inject the sample into the column with an elution volume 1.5 column volumes. The eluent was collected in 94 fractionation tubes each containing 5.2 mL fractions. The Bio-Rad assay was used to test for protein containing fractions while 15% SDS-PAGE was performed to analyze the purity of the fractions containing WLN6 protein. All the pure fractions were pooled together and concentrated on Amicon device fitted with a YM3 membrane to 2 mL. The sample was then stored at -80^{o}C.

Sample preparation for Nuclear Magnetic Resonance

2 mL of WLN6 protein pure stock solution (0.2 mM) was aliquoted, reduced by addition of excess DTT and degassed with nitrogen gas. The sample was then transferred to a nitrogen atmosphere and vacuum atmosphere glove box. The sample was then exchanged to 100 mM sodium phosphate buffer, pH 7.2, using an Amicon device fitted with a YM3 membrane. The WLN6 protein solution was then finally concentrated down to 540 uL. This volume was pipetted into a microcentrifuge tube to which 60 μL of D_2O was added. The total volume of the sample was 600 uL (10% D_2O) with a concentration of 0.5 mM. The sample concentration was estimated with the Bio-Rad assay. The prepared 0.5 mM WLNP protein sample was transferred to an NMR tube, capped with a septum cap and brought out of the anaerobic chamber. The sample was the shipped to Italy at the Centre for Magnetic Resonance, University of Florence.

Isotopic labeling of WLN6 protein

Isotopic labeling of proteins is important in solving solution structures using NMR. In two dimensional and three dimensional NMR studies, proteins are labeled with C-13 and/or N-15. For uniform labeling of WLN6 protein with ^{15}N and ^{13}C, the same expression vector used for overexpressing unlabelled WLN6 was used. The cells were incubated in minimal growth media (enriched phosphate buffer, pH 7.2). Just prior to labeling, a test induction for WLN6 protein was carried out in minimal media to analyze the protein expression levels in this media. ^{15}N labeled WLN6 protein was produced by growing Rosetta cells with pPOWD6 recombinant plasmid in minimal media supplemented with $^{15}NH_4Cl$ as a ^{15}N nitrogen source. 1 L of minimal media contains 6 g

of Na_2HP0_4, 3 g of KH_2PO_4, 0.5 g NaCl, 1 g of $^{15}NH_4Cl$, 0.4% dextrose sugar, 2 mM $MgSO_4$, 0.1 mM $CaCl_2$, 2 mL of 0.2% thiamin and 30μg/mL kanamycin sulfate.

The procedure for ^{15}N WLN6 protein expression was carried out as follows: A 5 ml LB culture treated in 30 μg/mL kanamycin was inoculated with Rosetta DE3/pPOWD6 plasmid colony and the cells were incubated at 37°C. When the OD_{600} of the medium was 0.8, the bacterial pellet was isolated and resuspended in the complete ^{15}N minimal media for further incubation. The cell culture was grown in a 2 L flask and the growth monitored with periodic measurement of OD at 600 nm. After the OD_{600} reached 0.6, protein expression was induced in 1 mM IPTG. The cells were harvested 6 hr later by centrifugation. The ^{15}N labeled protein was recovered by freeze-thaw extraction, anion exchange chromatography and finally gel filtration as outlined in the purification protocol explained earlier in chapter 2. This protein was also prepared for NMR studies as and shopped to CERM, Italy for NMR analysis. The ^{15}N and ^{13}C WLN6 protein was produced using a similar procedure but ensuring that the minimal growth media contained 1 g of $^{15}NH_4Cl$ per liter and 2 g of ^{13}C glucose per liter.

Determination of WLN6 protein concentration

Protein concentration of WLN6 protein was determined by a combination of Bradford Assay (Bio-Rad) and UV-Vis technique. In Bio-Rad assay, immunoglobulin G (*Ig*G) standard protein concentrations were prepared (ranging from 1.51 to 21.14 μg/mL). The corresponding UV absorbance at 595 nm of each IgG standard prepared was determined and the absorbance value was plotted as a function of IgG concentration. The resultant calibration curve was used to determine the concentration of pure WLN6 protein.

Site-directed mutagenesis of WLN6 protein

In order to compare the wildtype WLN6 protein with the mutant WLN6(G591D), mutagenesis was performed on the recombinant vector (pPOWD6). The Strategene Quick-change site-directed mutagenesis kit was used to introduce the G591D mutation. The sequence of the forward mutagenic primer was : 5' CTC ACG AGG ACA AAT GAC ATC ACT TAT GCC TCC G – 3' and the sequence of the reverse mutagenic primer was : 5' CGG AGG CAT AAG TGA TGT CAT TTG TCC TCG TGA G – 3'(underline indicates the point at which mutation was introduced). The following reagents were mixed in a 1 mL microcentrifuge tube: 30.9 μL double-deionized water, 5.0 μL Strategene 10x reaction buffer, 1.0 μL (20 ng) recombinant pJK1-62(1c) vector, 6.0 μL (125 ng) forward primer, 6.1 μL(125 ng) reverse primer, 1.0 μL Strategene dNTP mix and 1.0 μL Strategene *PfuTurbo* DNA polymerase. The solution was overlaid with 30 μL of mineral oil and subjected to the PCR.

Digestion of DNA by *Dpn1* enzyme

After the reaction mixture was subjected to several PCR cycles, the non-mutated parental DNA was digested with *Dpn1* restriction enzyme (10U/μL). 1.0 μL of the restriction enzyme was added to the PCR product. The reaction mixture was then centrifuged at 10,000 rpm for 1 minute in an eppendorf microcentrifuge. The mixture was then incubated at 37°C for 1 hr.

The mutated plasmid from the reaction above was transformed into DH5α *E. coli* cells according to the transformation protocol outlined earlier. The transformation product was plated on LB agar plates treated with 30 μg/mL kanamycin and incubated in

37°C overnight. A few colonies obtained from the transformation were inoculated in a starter culture, 5 mL which was then transferred to a 100 mL LB culture for plasmid recovery. The pure plasmid, pPOWD6-G591 was recovered after isolation and purification using Qiagen mini elute protocol.

Transformation and protein expression

The purified mutant plasmid (pPOWD6-G591D) was transformed into Rosetta (DE3) cells using the same methods described for wildtype pPOWD6 transformation. WLN6 (G591D) protein expression was studied via a time-course induction test in 1 mM IPTG (a synthetic mimic of the natural inducer, 1, 6- allolactose which binds to the *lac* repressor) on the 100 mL LB culture inoculated with mutated WLN6 plasmid (WLN6-G591D). 500 μL aliquots of samples were withdrawn every 30 min. and centrifuged for 15% SDS-PAGE induction analysis. After 4 hr of induction, the culture was harvested by centrifugation at 6000 x g for 15 min. The cells were stored in -20°C overnight for WLN6(G591D) protein extraction. The centrifuged aliquoted samples were analyzed by SDS-PAGE for induction.

Freeze/Thaw extraction of WLN6(G591D)

Freeze/Thaw extraction buffer was 20 mM MES/Na, 1 mM EDTA, 10 mM DTT, pH 6. The WLN6(G591D) protein bacterial pellets were resuspended in the freeze-thaw extraction buffer (24 mL of buffer per liter of induction culture). The suspension was gently agitated in ice for 1 hr. The non-soluble portions of the cells were pelleted by centrifugation at 6000 g for 15 minutes. Both the supernatant and the pellet were tested with analytical SDS-PAGE for the mutant WLN6-G591D protein. Since the mutant

protein was absent in the supernatant and present in the bacterial pellets, another extraction technique was used to solubilize the protein.

Extraction of WLN6(G591D) by sonication

E. coli Rosetta (DE3) cells containing WLN6(G591D) protein were resuspended in the freeze/thaw extraction buffer, pH 6, and vortexed for 3 min. The suspension was then subjected to sonication for 15 min. (five 1 min. pulses at 3 min. intervals). After sonication the suspension was subjected to continuous shaking at 70 rpm for 2 hrs. The extract was centrifuged at 6000xg for 15 min. Both the supernatant and the pellet were saved and analyzed for WLN6(G591D) protein with 15% SDS-PAGE.

Extraction of WLN6(G591D) by commercial detergent

BugBuster® protein extraction reagent is formulated for the gentle disruption of the cell wall of *E. coli* to liberate recombinant proteins. It provides a simple, rapid, low-cost alternative to mechanical methods such as French press or sonication for releasing expressed target protein in preparation for purification or other applications. The proprietary formulation utilizes a detergent mix that is capable of cell wall perforation without denaturing protein.

The bacterial pellet from the sonication procedure was resuspended in 12.5 mL BugBuster® reagent (5 mL per gram of cells). To reduce the viscosity of the lysate, 1 μL (25 U) benzonase nuclease per ml BugBuster® reagent was added into the suspension. 12.5 μL of protease inhibitor (1 μL per mL of BugBuster® reagent) was also added to the mixture. The cell suspension was incubated on a shaking platform at 50 rpm for 30 min at room temperature. Insoluble cell debris was removed by centrifugation at 16,000xg for

20 min. at 4°C. A 15% SDS-PAGE was performed on samples from both the supernatant and the pellet to determine the extraction efficiency and protein solubility in the reagent. The pellet and supernatant were stored at -20°C.

Solubilization of WLN6(G591D by guanidinium chloride

Because the mutant WLN6(G591D) was still in the pellet (15% SDS-PAGE) even after a series of extractions with different techniques, complete solubilization of bacterial cells was necessary. The test protocol for this extraction was developed as follows: 2.5 g of bacterial pellet containing WLN6(G591D) was resuspended in 10 mL of 8 M guanidinium chloride (2.5 mL/gram of pellet). The suspension was placed on ice and gently agitated until solubilization was complete. The solubilized suspension was centrifuged at 12,000xg for 30 min. and the supernatant was isolated. The supernatant was slowly diluted in freeze-thaw extraction buffer (20 mM MES/Na, pH 6, 0.1 mM EDTA, 10mM DTT) 40 fold. This mixture was filtered through a 0.22 μm protein filter membrane. The filtered extract was then concentrated to 10 mL using an Amicon device fitted with a YM3 membrane. An analytical sample of this extraction process was subjected to SDS-PAGE.

Extraction of mutant WLN6(G591D) with various buffers

Since the solubility of mutant WLN6(G591D) was low (WLN6(G591D) was poorly extracted), different buffers at different conditions were prepared to optimize the extraction conditions for the mutant protein. Below is a list of solutions that were prepared to enhance the mutant protein extraction.

- ✓ 20 mM MES/Na, pH 5.5, 0.1mM EDTA

- ✓ 20 mM MES/Na, pH 6.5, 0.1 mM EDTA
- ✓ 20 mM MES/Na, pH 6.2, 0.1 mM EDTA, 100 mM NaCl
- ✓ Bugbuster® Extraction Reagent (Tris/Cl, pH 7.2)
- ✓ 8 M Guanidine Hydrogen Chloride, pH 6

A test extraction was carried out in 5 different microcentrifuge tubes. First, the same amount (0.1 g) of bacterial pellet containing mutant WLN6(G591D) protein was transferred to all the 5 microcentrifuge tubes. 20 μL of each reagent was added to the corresponding pellet. Pellet in each tube was resuspended in the buffer after which the suspensions were vortexed for 3 minutes each. The tubes were then placed in a slow shaker for 10 min. and then centrifuged in a microcentrifuge for 2 min at 14,000 rpm. The supernatant in each tube was saved and analyzed with SDS-PAGE.

Site-directed mutagenesis of G591D in the two domain construct WLN5-6

Since all attempts to extract mutant WLN6(G591D) protein were not successful, we decided to attempt the same mutation (G591D) in a two domain construct, WLN5-6. Our hypothesis was that the same mutation in WLN5-6 would enhance the stability of the mutant protein. This hypothesis was based on the earlier experience with WLN5-6.

Mutagenesis was performed on the recombinant vector pDAWD5-6. The Strategene Quick-Change Site-Directed Mutagenesis kit was used to introduce the G591D mutation. The sequence of the forward mutagenic primer was: 5' CAA CCA GAG CCA TGG CAC CGC AGA AG- 3' and the sequence of the reverse mutagenic primer was: 5' CGG AGG CAT AAG TGA TGT CAT TTG TCC TCG TGA G – 3' (underline indicates the point at which mutation was introduced). Mutagenesis was

performed using Strategene kit following the Strategene protocol. The reaction mixture was finally subjected to the PCR.

After the reaction mixture was subjected to several PCR cycles, the non-mutated parental DNA was digested with *Dpn1* restriction enzyme (10U/μL). The mutated plasmid from the reaction above was transformed into XL-Gold ultracompetent cells as outlined below. The plates were then incubated overnight at 37°C. The colonies obtained from transformation were inoculated in LB and the plasmid recovered as using Qiagen midi prep procedure outlined in the Qiagen protocol. The plasmid was confirmed by agarose gel electrophoresis and the concentration determined by UV-Vis spectrophotometer. This was done by measuring the absorbance at 260 and 280 nm wavelengths respectively. The purified plasmid (800 ng of pWD5-6(G591D) was then availed for sequencing in Dr. Barkman's Lab. 2 μL of the plasmid was transformed in Rosetta (DE3) cells for induction test using the same methods described earlier. Protein expression was studied via a time-course induction test using 1 mM IPTG on the 100 mL LB culture inoculated with mutant WLN5-6 plasmid (pWD5-6-G591D). 250 uL aliquots of samples were withdrawn every 30 minutes and centrifuged to be analyzed for induction. After 4 hrs of induction, the culture was harvested by centrifugation at 6000xg for 15 min. The cells were stored in -20°C overnight for WLN5-6 protein extraction. The centrifuged aliquoted samples were analyzed by SDS-PAGE for induction.

Extraction of mutant WLN5-6(G591D)

Protein extraction was done according to the procedure previously described using freeze-thaw extraction buffer (20 mM MES/Na, pH 6, 0.1 mM EDTA, 10 mM

DTT). Also BugBuster® test extraction was carried out using similar protocol explained earlier. These two extraction methods were compared by 15% SDS-PAGE.

Ligation independent cloning (LIC)

Due to low yields of WLN5-6(G591D), we decided to clone the mutant plasmid as a fusion protein following the protocols described by Novagen. Fusion proteins are known to improve protein solubility and also enhance protein purification. The sense primer was designed to encode the last four amino acids of the enterokinase (EK) cleavage site plus the C-terminal flanking amino acid Met. The sequence of the GST fusion forward primer was: 5'- GAC GAC GAC AAG ATG GCA CCG CAG AAG TGC TTC TTA CAG – 3' and the sequence for the GST fusion reverse primer was: 5'- GAG GAG AAG CCC GGT CTA CTG GGC CAG GGA AGC ATG AAA G – 3'. The forward primers for the thioredoxin fusion protein was: 5'- GGT ATT GAG GGT CGC ATG GCA CCG CAG AAG TGC TTC TTA CAG -3' while the reverse primer for thioredoxin fusion protein was: 5'- AGA GGA GAG TTA GAG CCC TAC TGG GCC AGG GAA GCA TGA AAG – 3'.

Two PCR tubes were set with the following: In the first tube 58 μL H_2O, 10 μL thermopol buffer (10x), 10 μL 2 mM dNTP mix, 10 μL Ek/LIC WLN5 Fwd primer (10 μM), 10 μL Ek/LIC WLN6 reverse primer (10 μM), 2 μL template (pWD56-G591D), and 0.9 μL DNA polymerase (Deep Vent). This mixture was overlaid with 40 μL mineral oil. In the second tube the following reagents were mixed together: 58 μL H_2O, 10 μL thermopol buffer (10x), 10 μL 2mM dNTP mix, 10 μL Xa/LIC WLN5 Fwd primer (10 μM), 10 μL Xa/LIC WLN6 reverse primer(10 μM), 2 μL template(pWD56-G591D), and 0.9 μL DNA polymerase (Deep Vent). The two tubes were set on a PCR machine and the

desired DNA piece amplified using the following PCR program: Melting temperature of 95°C for 5 min, annealing temperature of 65°C for 1 minute, extension temperature of 72°C for 40 sec, melting at 95°C for 40 sec, annealing of at 65°C for 1 min and Extension at 72°C for 1 min. The last 3 cycles were repeated 27 times.

After the DNA amplification, an agarose gel electrophoresis was run to ascertain the presence of the DNA piece. The PCR product was then purified using Qiagen mini elute protocol. The purified product was also quantified by agarose gel electrophoresis

T4 DNA polymerase treatment of target insert

T4 DNA polymerase treatment of the insert was performed to generate compatible overhangs on the insert. The following components were assembled in a PCR tube: 10 μL purified PCR product, 2 μL T4 DNA polymerase buffer (10x), 2 μL 25 mM dATP, 1 μL 100 mM DTT 0.4 μL T4 DNA polymerase (LIC-qualified) and 4.6 μL nuclease-free water. The total volume of the components was 20 μL. The reaction was started by adding the enzyme and stirring with the pipette tip for 2 minutes. The mixture was then incubated at 22°C for 30 min. Finally the temperature was raised to 75°C for 20 min. to inactivate the enzyme.

Annealing the vector and the treated insert (Ek/LIC WLN5-6(G591D)

Annealing of the pET41 LIC vector and the treated insert (Ek/LIC WLN5-6(G591D) was done by assembling the following components in a sterile PCR tube: 1 μL Ek/LIC vector (pET 41) and 2 μL T4 DNA polymerase-treated Ek/LIC WLN5-6(G591D) insert. These were incubated at 22°C for 5 min then 1 μL 25 mM EDTA was added to the mixture with stirring followed by incubation at 22°C for 5 min. Annealing continued for

1 hr. The same process was performed for Xa/LIC WLN5-6(G591) insert. However, the annealing vector used was pET32 instead of pET41.

The DNA clones produced were sequenced in Dr. Barkmans Lab. 20 ng of both plasmids (pEk/LIC WLN5-6(G591D) & pXa/LIC WLN5-6(G591D) were transformed in Nova Blue Giga Singles ^{TM} competent cells according to the protocol in the Novagen kit. The transformation products were plated on LB plates treated with kanamycin (30 μg/mL, for pEk/LIC WLN5-6(G591D) and/or ampicillin (100 μg/mL, for pXa/LIC WLN5-6(G591D). The plates were incubated at (37°C) for 24 hr.

Some of the observed colonies were inoculated in different 5 mL LB treated with 30 μg/mL kanamycin or 100 μg/mL ampicillin. The cultures were grown to a high density and transferred to a 100 mL culture for plasmid isolation. The cultures were harvested by centrifugation followed by plasmid isolation and purification according to the Qiagen Midi-Prep protocol explained earlier. Some of the plasmid was submitted for sequencing in Dr. Barkmans Lab, but the sequencing reaction repeatedly yielded overlapping products. Later, it was determined by sequencing at Retrogen that an insertion product within the gene occurred. This was not determined prior to subsequent experiments and expression studies of this construct. Nonetheless, valuable information was learned about expression and purification of the mutant protein. Now, studies are being performed on the corrected sequence; however, these studies are not described in this thesis.

Transformation of LIC plasmids (uncorrected sequence – vide supra)

Both plasmids were transformed in Rosetta (DE3) pLys cells. The product was plated on LB in 30 μg/mL kanamycin and incubated overnight at 37°C. Some of the positive colonies observed on the plates were inoculated and tested for protein induction. The induction was done with addition of 1 mM IPTG and this was continued for 4 hrs. The bacterial pellets were harvested by centrifugation at 6000xg and stored at -20 °C. The samples withdrawn at each hr interval were analyzed by SDS-PAGE.

Restriction analysis

To verify cloning, restriction analysis was carried out by assembling the following reagents in one tube: 10 μL of purified plasmid (pEk/LIC WLN5-6(G591D) or pXa/LIC WLN5-6(G591D), 0.8 μL BglII, 0.2 μL BamHI, 0.2 μL, 10x Bovine Serum Albumin (100 mg/mL)), 0.2 μL BamH1 buffer and 8.8 μL H_2O. This mixture was incubated at 37°C for 12 hr. An analytical sample was run in agarose gel to confirm digestion.

Extraction and purification of fusion proteins (GST-WLN5-6(G591D) and Thioredoxin-WLN5-6(G591D)

The fusion mutant protein-containing bacterial pellets were thawed and resuspended in BugBuster® extraction buffer. The extraction of the fusion proteins was done with BugBuster® according to the protocol explained in chapter two. The extracts (supernatant) were tested for the respective mutant fusion proteins (GST fusion and Thioredoxin fusion) by estimation of the combined masses (fusion tag and mutant protein) on an SDS-PAGE. Solubilization of bacterial pellets containing GST and Thioredoxin-WLN5-6(G591D) proteins were done in 6 M guanidinium chloride for total protein recovery. GST fusion protein, GST-WLN5-6(G591D) was then exchanged

slowly in GST binding buffer (140 mM NaCl, 2.7 mM KCl, 10 mM Na_2HPO_4 1.8 mM KH_2PO_4, pH 7.3) using an Amicon device fitted with a YM3 membrane. This mutant protein was then subjected to affinity purification step - GST Column purification. The GST column was pre-packed from Amersham Inc. with glutathione resin. The column was integrated to the Amersham FPLC machine and equilibrated with 2 column volumes (40 mL) of GST binding buffer (140 mM NaCl, 2.7 mM KCl, 10 mM Na_2HPO_4, 1.8 mM KH_2PO_4, pH 7.3). The sample was injected to the GST column. This was followed by 2 column volumes wash of the column with GST-binding buffer and then isocratic elution with 5 column volumes (100 mL) of GST elution buffer (50 mM Tris, 100 mM reduced glutathione, pH 8). During elution, fractions were collected in tubes and analyzed by the Bio-Rad assay and SDS-PAGE for protein and mutant fusion protein (GST-WLN5-6(G591D) respectively. Thioredoxin fusion protein extract, Thio-WLN5-6(G591D), was also loaded onto the Histidine Tag column after equilibration with 2 column volumes of HisTag binding buffer (20 mM sodium phosphate buffer, 0.5 M NaCl, 20 mM Imidazole, pH 7.4). The protein was then eluted with 3 column volumes (60 mL) of HisTag elution buffer (20 mM sodium phosphate buffer, 0.5 M NaCl, 500 mM Imidazole, pH 7.4). The elution volume was collected in different 2 mL fractions and analyzed using Bio-Rad assay and SDS-PAGE.

Enterokinase cleavage of GST-WLN5-6(G591D)

A test cleavage of the GST tag from the mutant protein was carried out by enterokinase cleavage enzyme (1U) by assembling the following in a microcentrifuge tube: 13 μL (50 μg) of GST fusion protein from GST purification (Ek/LIC WD56-G591D), 13 μL of 1x Enterokinase cleavage buffer, and 1 μL of porcine enterokinase

(1U). This mixture was incubated at 25°C for 18 hr. Samples (cleaved and uncleaved) were analyzed using SDS-PAGE. Similar conditions employed for the test cleavage were duplicated for the entire 10 mL volume (3.5 μg/mL) of GST-purified protein sample. All samples were analyzed by15% SDS-PAGE.

Factor Xa cleavage of thioredoxin-WLN5-6(G591D)

Cleavage of the thioredoxin fusion tag from the mutant protein was carried out by Factor Xa cleavage enzyme by assembling the following reagents in a microcentrifuge tube: 13 μL (50 ug) of thioredoxin fusion protein from HisTag purification (Thio-WLN5-6(G591D), 13 uL of 1X Factor Xa cleavage buffer and 1 μL of Factor Xa enzyme (1U). This mixture was incubated at 25°C for 18 hr. Samples (cleaved and uncleaved) were analyzed by SDS-PAGE. Similar conditions employed for the test cleavage were duplicated for the entire volume (7.5 mL) of His-Tag-purified protein sample with adjusted quantity ratios of reagents.

Transformation of mWD4-Avitag in Rosetta ™ (DE3) cells

Single molecule studies of WLN4 are being carried out in the laboratory of Professor Peng Chen at Cornell University. Using our expression system, Dr. Chen's laboratory added an Avitag to the protein. Details of this process and the sequence can be obtained in writing from Professor Chen. In order to purify this protein, 1 μL of the mWD4-Avitag labeled sample (48.9 ng/μL) was transformed in Rosetta™(DE3) cells. The cells were plated on LB containing 30 μg/mL kanamycin. The plates were incubated at 37°C overnight.

Protein induction (mWD4-Avitag)

5 mL LB (containing 30 μg/mL) in a culture tube was inoculated with a colony from the previous transformation. The culture was grown in a shaker at 37°C and the OD_{600} was monitored. The 5 mL culture was then transferred to a 1 L LB treated with 30 μg/mL kanamycin. The OD_{600} was monitored until 0.6 after which induction was initiated in 1 mM IPTG .The induction process was continued for 4 hr with successive withdrawal of a 500 μL sample after every 1 hr. After induction was complete, the bacterial cells were harvested by centrifugation at 6000xg for 20 min. The samples were subjected to SDS-PAGE for analysis. The pellets were stored at -20°C.

Extraction and purification of mWD4- Avitag

Freeze/thaw extraction

The bacterial cells containing mWD4-Avitag protein were subjected to 3 cycles of freezing and thawing in liquid nitrogen and water respectively. 25 mL of Freeze/thaw extraction buffer (20mM MES/Na, 10mM DTT, 1mM EDTA, pH 6) was used to resuspend the thawed cells. The suspension was shaken (100 rpm) for 30 min (to enhance protein extraction). mWD4-Avitag protein was finally recovered in the supernatant after centrifugation at 6000xg for 20 min. The supernatant was filtered through a 0.22 μm filter membrane.

Anion exchange chromatography

Buffers were prepared and filtered in a 0.22 μm filter. The buffer compositions were as shown below:

- Low salt buffer - 20mM MES/Na, pH 6, 10mM DTT
- High Salt buffer - 20mM MES/Na, pH 6, 10mM DTT, 1M NaCl
- Column used: DEAE Sepharose

mWD4-Avitag sample was loaded onto the DEAE column integrated with FPLC. The sample was eluted with a linear salt gradient. The fractions containing mWD4-Avitag were collected in tubes. The fractions containing the protein (mWD4-Avitag) were analyzed with SDS-PAGE.

Sample concentration and gel filtration

The DEAE fractions containing mWD4-Avitag were collected and concentrated using a YM3 membrane to a final volume of 3 mL. This volume was loaded onto a large superdex column (330 mL Column Volume) for further purification and separation. Pure fractions were collected and analyzed by SDS-PAGE.

Mass Spectroscopy (ESI-MS) of mWD4-Avitag

A pure protein sample of the m-WD4 Avitag protein was submitted to the University of Michigan, Protein Structure Facility for Mass spectrometry. 200 μL of gel filtration sample (fraction 39) was diluted with water 3 fold. The volume (600 μL) was concentrated to 50 μL using microcon fitted with YM3 membrane. The composition of the final sample submitted for mass spectrometry was as follows: Buffer components: 6

mM MES/ Na, 50 mM NaCl, 3 mM DTT, pH 7, Volume: 40 uL and Concentration: 0.49 mM.

NMR spectroscopy

The strategy used for the determination of solution NMR structure of WLN6 involved careful preparation of unlabeled and labeled protein solutions, spectra acquisition, spins system and sequential resonance assignment, collection of conformational constraints and calculation of the 3D structure. Spin system resonance assignment identified which proton resonance belonged to which residue type while sequential resonance assignment showed which proton belonged to which residue in the WLN5-6 protein sequence. The calculated NOE and J-coupling NMR constraints were used to identify which protons were close in space and what the torsion angles were. The structure calculated represents conformation(s) consistent with all the NOE, J-coupling and other constrains. The reported structure is a mean of an ensemble of 20 lowest energy structures of the protein calculated from the collected data. All NMR experiments were performed at the Magnetic Resonance Center (CERM), University of Florence, Italy. WLN6 NMR spectra were acquired on Avance 900, 800, 600 and 500 Bruker Spectrometers operated at a proton nominal frequency of 900.13 MHz, 800.13 MHz, 600.13 MHz and 500.13 MHz respectively. All 2D and 3D spectra were collected at 298 K, processed using the standard Bruker software (XWINNMR) and analyzed using the CARA program. $^{1}H,^{15}N$-Heteronuclear single quantum coherence (HSQC) experiment. The $^{1}H,^{15}N$-HSQC experiment is a two dimensional (2D) experiment that depends upon scalar coupling between the amide nitrogens and their attached protons. Each of the naturally occurring amino acids (except proline) gives one resonance from $^{1}H,^{15}N$-HSQC

spectrum which corresponds to the N-H amide group. The spectrum contains the signal of the H_N protons in the protein backbone and since there is only one backbone H_N per amino acid, each HSQC signal represent one single amino acid.

Resonance assignment and structural restraints

^1H - ^1H distances and the dihedral angles were determined through Nuclear Overhauser Effect spectroscopy (NOESY) and HNHA experiments. H-bond constraints were obtained using transverse relaxation optimized spectroscopy (TROSY) version of the long range HNCO experiment at a magnetic field of 700 MHz. Relaxation experiments were performed on a Bruker Avance 600 MHz NMR at 298 K. The WLN6 structure and folding was calculated from the constraints derived from these experiments.

Relaxation rate measurements

The relaxation experiments were performed on Bruker Avance 600 MHz or 500 MHz spectrometers at 298 K. ^{15}N R_1, R_2, and steady-state heteronuclear ^1H,^{15}N NOEs were measured with pulse sequences as described by Farrow *et al.* (Farrow *et al.*, 1995). Integration of cross peaks for ^{15}N R_1, R_2, and ^1H, ^{15}N NOEs spectra was performed by using the standard routine of the XWINNMR program. Relaxation rates R_1 and R_2 and heteronuclear NOE values were determined following a standard procedure as reported previously (Arnesano *et al.*, 2001). The experimental relaxation rates were used to map the spectral density function values, J(£sH), J(£sN), $J_{eff}(0)$, following a procedure available in literature (Peng & Wagner, 1992), in order to investigate the backbone motions. An estimate of the overall rotational correlation time was derived from the measured R_2/R_1 ratio by using a standard procedure (for example, see (Arnesano *et al.*,

2001).

Circular Dichroism

A circular dichroism (CD) experiment was used to probe helicity of WLN5-6(G591D). A WLN5-6(G591D) solution was prepared by reduction in 10 mM DTT and then exchanging in 50 mM sodium phosphate, pH 7.2 buffer under anaerobic conditions. The final sample had a concentration of 12.5 μM WLN5-6(G591D). A 10 mm jacketed cell was thoroughly cleaned and dried before samples were introduced. The spectropolarimeter was attached to a nitrogen generator. Temperature was set and maintained at 25°C by running water through a jacketed cell. After 1 hr of incubation the samples were scanned at a speed of, starting with the blank, at a rate of 20 nm per second over the far UV range of 190 nm to 300 nm. CD spectra were collected on a J-80 spectropolarimeter (JASCO-J-80, Japan) fitted with a 150 W Xenon lamp. The spectrum was corrected for background noise.

CHAPTER III

RESULTS

Cloning of WLN6

The portion of the WLNP gene encoding for the N-terminal metal binding domains 6 was amplified from a human cDNA plasmid encoding full length WLNP through 28 PCR cycles in a MiniCycle using Deep Vent DNA polymerase (New England Biolabs). PCR products were purified, double digested with restriction endonucleases Nco1 and BamH1 then cloned into an *E. coli* expression vector, pET24d. The recombinant plasmid was transformed in DH5α cells and the recombinant plasmid was isolated and purified (see Fig 5)

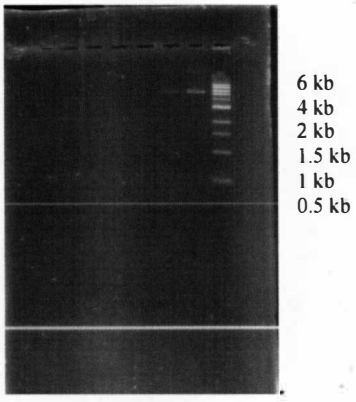

Figure 5. Agarose gel electrophoresis of WLN6 recombinant pure plasmid on a 1 % agarose gel. Lane1, is the 1 kb marker, lanes 2 & 3 are recombinant plasmid (~5,500b p)

Cloning was verified by sequencing of the gene in Dr. Barkman's lab and also by restriction analysis of the recovered plasmid employing BamHI and NcoI restriction enzymes. The sequence of the insert matched with the native sequence for this portion of the gene. The alignment was done using the DNA Strider program. Band representing a fragment ~250 base pairs (bp) was observed on a 1% agarose electrophoresis gel of the

doubly digested recombinant plasmid. This was a confirmation that WLN6 gene was successfully inserted into the expression vector, pET24d.

Induction of WLN6 in LB media

The time course induction of WLN6 protein was done to test the efficiency of WLN6 protein expression in LB media containing 30 µg/L of kanamycin. The recombinant plasmid (pPOWD6) was transformed into *E. coli* Rosetta (DE3) cells and induced for WLN6 protein expression in LB medium using IPTG. Kanamycin was used to select for cells transformed with the recombinant plasmid because the plasmid contained genes for kanamycin resistance. The growth of the cells was monitored by measuring optical density at 600 nm (OD_{600}). WLN6 expression was induced at OD_{600} of 0.6 by addition of 1 mM IPTG. IPTG binds and inactivates the *lac operon* repressor and therefore induce WLN6 gene transcription by RNA polymerase. The OD_{600} was measured periodically until completion of protein induction (~ 4 hrs). The samples withdrawn in every time interval were centrifuged and analyzed on SDS-PAGE gel for WLN6 induction. The loading on SDS-PAGE was normalized by the OD_{600} reading using equation 3.1.

$$\frac{OD_{600} \text{ at time } 0 \times 15\ \mu l}{OD_{600} \text{ at time } t_i} \qquad 3.1$$

The results showed a steady increase in cell density with time (this is indicated by subsequent increase in OD_{600}) (Table 4). The bacterial cells growth was not hampered by addition of IPTG, instead there was a gradual growth of cells in the nutrient medium (LB). The normalized loading on SDS-PAGE showed increase in intensity, with time, of

a protein band of ~7.5 kDa believed to be of WLN6 protein (Figure 6). This shows that WLN6 induction and expression was successful. A 10 L batch was planned to produce more protein.

Time(min)	Optical Density (OD_{600})	Normalized loading vol.(μL)
0	0.6341	15.00
30	1.0530	9.030
60	1.3780	6.900
90	1.6060	5.920
120	1.7057	5.570
150	1.8262	5.208
180	1.9675	4.830
210	2.0161	4.710
240	2.1310	4.460

Table 1. Time-course induction of WLN6 protein showing steady increase in OD_{600} with time. The last column shows the amounts normalized by OD_{600} for loading on SDS-PAGE.

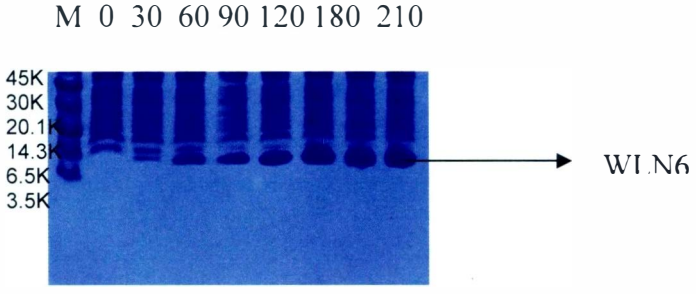

Figure 6: 15% SDS-PAGE showing induction and expression of WLN6 protein in 1 mM IPTG with increase in time. Time is shown in min.

Production of a 10 L batch of WLN6 protein

From the successful test induction and expression of native WLN6 protein, a 10 L batch was produced in LB media containing similar concentration of kanamycin following the protocol outlined earlier. The aim was to produce native WLN6 protein in sufficient quantities for characterization. The cells were pelleted by centrifugation then extracted for WLN6 protein by the freeze-thaw method. After harvesting and extraction, the WLN6 crude extract was analyzed by SDS-PAGE. A strong band on SDS-PAGE gel of about 7.5 kDa showed that WLN6 protein was expressed well in the 10 L batch.WLN5-6 was successfully extracted using the freeze-thaw method and isolated by a two step purification scheme involving anion exchange chromatography and gel filtration chromatography.

Purification of WLN6

Anion exchange chromatography

The freeze/thaw WLN6 extract was filtered then loaded onto a pre-equilibrated DEAE Sepharose anion exchange column (Amersham Pharmacia Biotech) to isolate it from other contaminating proteins. Proteins that bear negative charge at pH 6 preferentially bind to the positively charged DEAE resin while the neutral and positively charged ones flow through without binding. The strength of binding of the proteins to the column partially depends on the charge on the protein. Those that bind weakly are eluted first at low ionic strength while those that bind strongly are eluted at higher salt concentrations. WLN6 has a pI of 5.01 and therefore bears net negative charge at pH 6 (pH of the solvent buffer). This protein should ideally bind to the DEAE Sepharose anion exchange column. Protein elution was monitored by the UV absorption profile at 254 nm.

Polypeptides absorb UV light strongly around this wavelength. However, other contaminant biomelecules like DNA and RNA also absorb UV light at the same wavelength. The resulting fractions were also analyzed by the BioRad protein assay to identify protein containing fractions and also to estimate protein concentration (Table 5). SDS-PAGE was done to identify WLN6-containing fractions (Figure 7). SDS-PAGE separates proteins based on size; the smaller proteins experience less resistance while moving through the gel pores compared to the larger ones and therefore move faster through the gel. To estimate the protein sizes more accurately, a set of protein standards of known molecular weights were also ran alongside the protein samples.

Sample	Total protein concentration(μg/mL)
Pre-filtration supernatant	2744
Post filtration supernatant	2464
Flow-Through fraction 1	29.92
Flow-Through fraction 2	238.4
Flow-Through fraction 3	238.4

Table 2: Protein concentration at various steps of anion exchange chromatography (DEAE) purification.

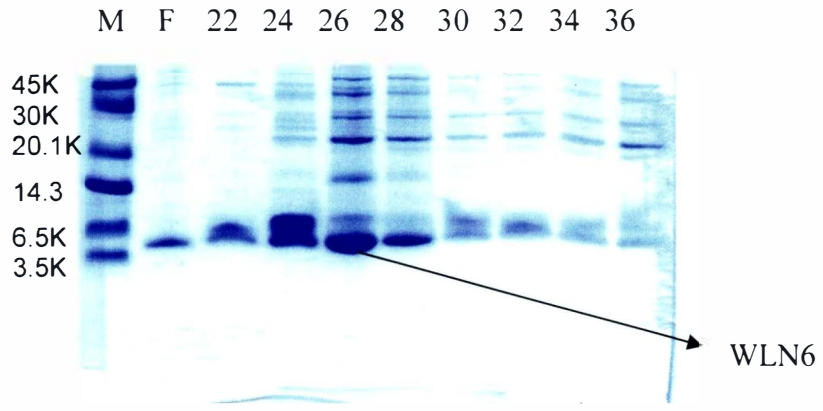

Figure 7. SDS-PAGE of Anion exchange (DEAE) fractions. M is the Rainbow low molecular weight marker, 22-36 are DEAE fractions, F is pre-filtered freeze-thaw extract. WLN6 band of ~7 kDa is present in fractions 22-36.

The BioRad protein assay showed that all the peak fractions contained protein but at varied concentrations. Fractions 22-36 had the highest concentration. SDS-PAGE analysis was used to identify WLN6-containing fractions. 10 μL were withdrawn from each of the peak fractions, mixed with loading dye and water and run on a 15% Tricine SDS-PAGE gel (Figure 7). The gel revealed that WLN6 eluted in fractions 22-36 which corresponded to about 20% salt concentration (0.2 M NaCl). The ion exchange chromatography concentrated WLN6 in fractions 22-36 but the SDS-PAGE revealed the presence of other proteins of different molecular weights. To further isolate WLN6, size exclusion chromatography (gel filtration) technique was used.

Gel filtration

This purification step was used to fractionate the proteins based on their sizes. The WLN6 containing fractions from AEC were concentrated down to 2 mL using an Amicon device fitted with a YM3 membrane. The concentrated protein solution was loaded onto a Superdex G75 10/30 gel filtration column (Amersham Pharmacia) pre-equilibrated with MES buffer (20 mM MES/Na, pH 6.0, 150 mM NaCl, 10 mM DTT).

SEC separates molecules based on size. Superdex G75 separates molecules in the range of 3 to 75 kDa. In SEC, the larger molecules elute first while the smallest in column range elute last. UV absorption at 254 nm was used to monitor elution of proteins. The BioRad protein assay was used to identify protein containing fractions. The WLN6-containing fractions were specifically identified by SDS-PAGE. Pure bands of ~ 7.5 kDa appeared on SDS-PAGE column between fractions 39-45 (Figure 8).

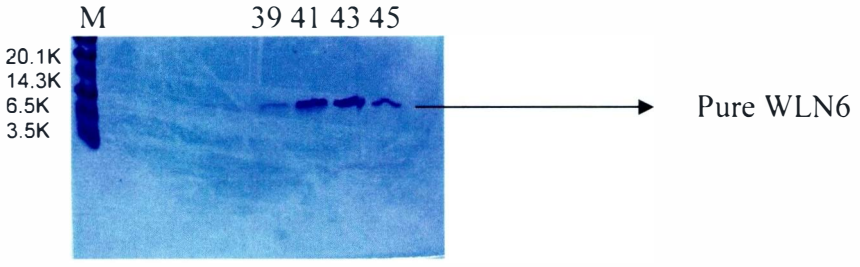

Figure 8: 15% Tricine SDS-PAGE of pure gel filtration fractions containing WLN6. M indicates the low molecular wt. rainbow protein marker.

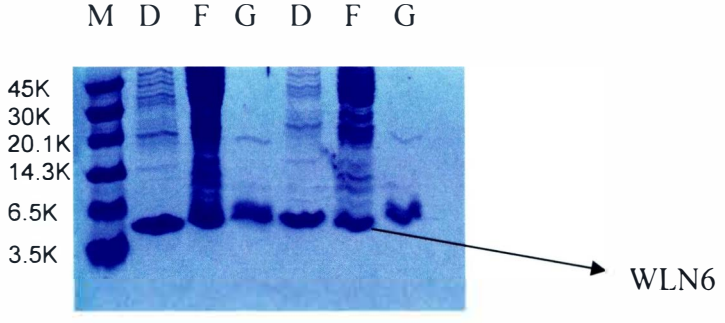

Figure 9: 15% SDS-PAGE showing various stages of WLN6 purification. M denotes protein marker. D, F and G are samples withdrawn after anion exchange purification, freeze-thaw extraction and gel filtration respectively.

Expression of mutant WLN6(G591D)

Strategene site-directed mutagenesis was successfully introduced on the native pPOWD6 template to replace glycine to aspartic acid at the amino acid residue 591 in the N-terminal domain of Wilson Protein (G591D). Correctly designed primers were used to introduce the mutation (G591D) and this was confirmed by DNA sequencing.

Recombinant mutant WLN6 Plasmid was transformed in DH5α cells (*E. coli*) cells and the plasmid isolated and purified (Figure 10 a). This plasmid was then transformed in Rosetta (DE3) cells, inoculated in LB and induced with IPTG for protein expression. Expression was analyzed by SDS-PAGE. (Figure10). WLN6(G591D) protein expression was successful. However, the protein could not be extracted from the bacterial cells after several trials with different buffers including solubilization with 8M guanidinium chloride. The point mutation probably interfered with the folding and thus stability of the protein.

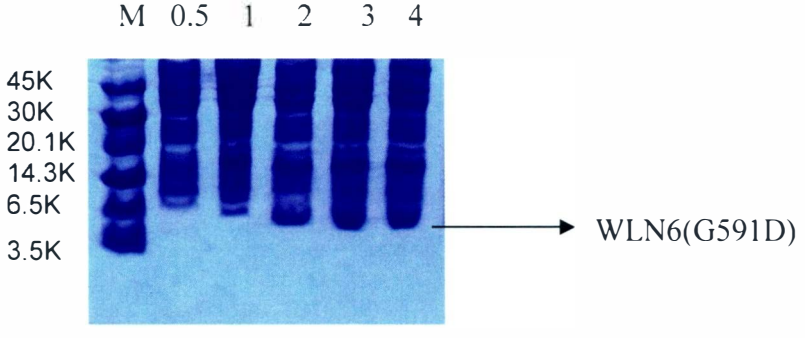

Figure 10: 15% SDS-PAGE showing a time-course induction of WLN6(G591D) protein in 1 mM IPTG (shown with arrow); induction time is shown in hr.

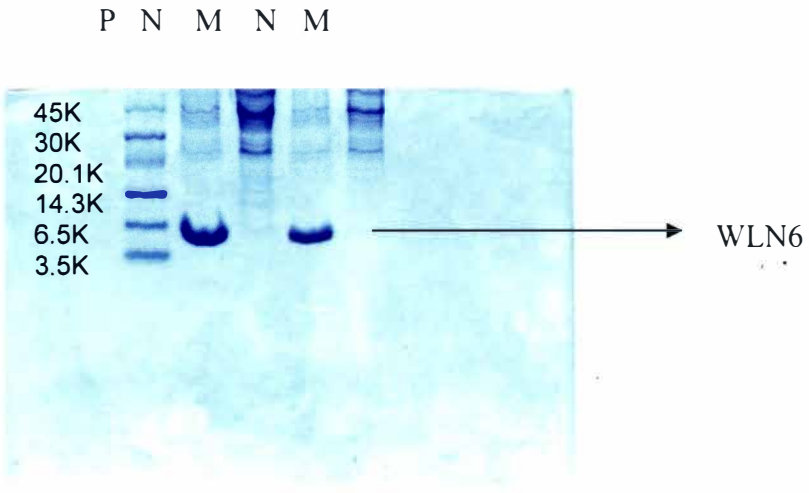

Figure 11: Comparison between solubility of WLN6 and WLN6(G591D) in extraction buffer (20 mM MES/Na, 10 mM DTT, pH 6). P is protein marker; N and M are native and mutant WLN6 respectively.

Another strategy was developed after observing the good stability of native WLN5-6 construct with varied concentrations of guanidinium chloride (GnHCl). Despite being a strong denaturant, WLN5-6 titrated with GnHCl was still stable in up to 3M GnHCl (H,^{15}N-HSQC experiments in Florence, Italy) (Most proteins are completely denatured in 2M GnHCl). Consequently, G591D mutation was successfully introduced in the double construct WLN5-6 gene. The G591D mutation was confirmed by DNA sequencing. The recombinant plasmid was transformed in Rosetta *E. coli* cells, inoculated in LB and the protein expressed in 1mM IPTG. The protein extraction levels were insignificant to obtain a desirable protein concentration for NMR studies.

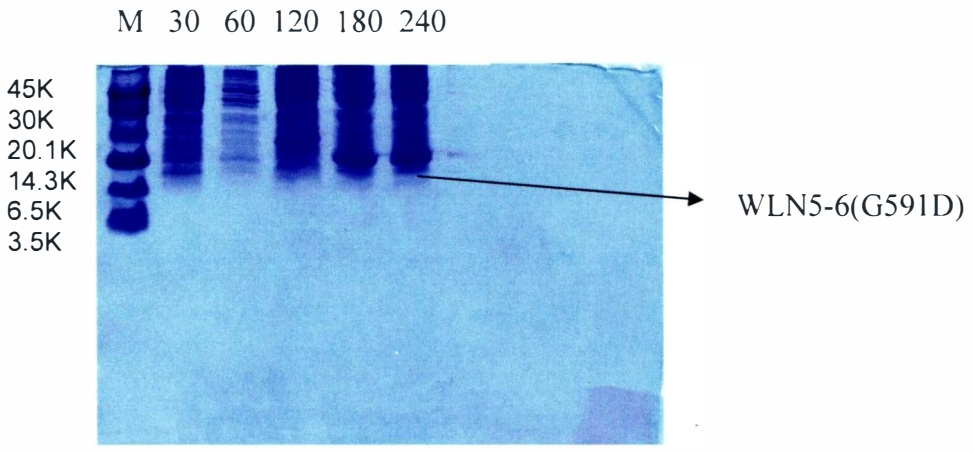

Figure 12: 15% Tricine SDS-PAGE showing a time-course induction of WLN5-6(G591D) mutant protein.

The third strategy was to improve the expression level of the mutant protein, WLN5-6(G591D). Proteins are known to express better when they are cloned in a fusion vectors. This strategy therefore employed the protocol of Ligation Independent Cloning (LIC) with vectors coding for glutathione transferase (GST) tag and thioredoxin tag. LIC vectors were created by treating a linearized backbone with T4 DNA polymerase in the presence of only one dNTP (dATP). The 3' to 5' exonuclease activity of T4 DNA polymerase removes nucleotides until it encounters a residue corresponding to the single dATP present in the reaction mix. At this point, the 5' to 3' polymerase activity of the enzyme counteracts the exonuclease activity to effectively prevent further excision. Plasmid sequences adjacent to the site of linearization are designed to produce specific noncomplementary 13- and 14-base single stranded overhangs in the LIC vector. PCR products with complementary overhangs were created by building appropriate 5' extensions into the primers. The PCR product was purified to remove dNTPs (and template plasmid) and then treated with T4 DNA polymerase in the presence of the appropriate dNTP to generate the specific vector-compatible overhangs. The annealed LIC vector and insert were transformed into competent *E. coli* cells. The positive clones

were transformed in Nova blue giga *E. coli* strains. Protein expression was induced with IPTG (Figure 13 A). The protein was expressed in fusion with GST and thioredoxin respectively. The fusion protein (GST-WLN5-6(G591D) was purified by affinity column (GST column) and eluted fractions collected for analysis (Figure 13 B).

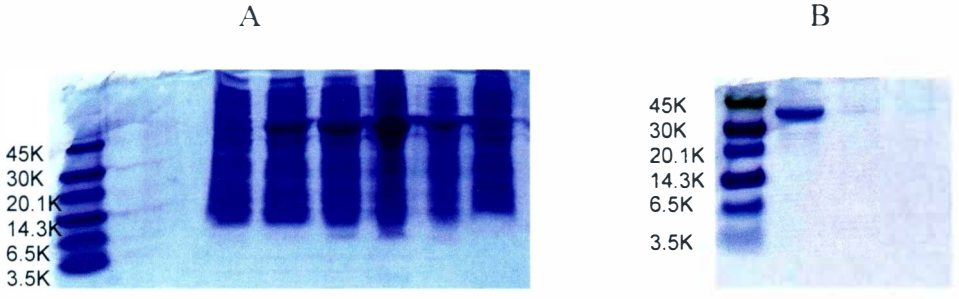

Figure 13. A: Time course protein induction of GST fusion protein, GST-WLN5-6(G591D). Protein induction is observed at ~ 45 kDa. B: GST purified fusion mutant protein.

Cleavage of the GST fusion tag

The GST and thioredoxin tags were cleaved using porcine enterokinase and Factor Xa respectively. Gel analysis showed a positive GST cleavage of mutant WLN5-6(G591D) and GST fusion tag both running at the correct masses in the SDS-PAGE. The cleavage for Factor Xa was not successful.

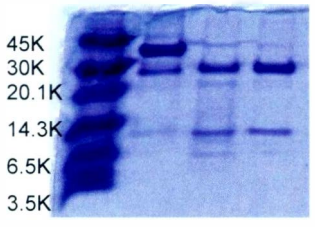

Figure 14: Porcine enterokinase cleavage of mutant GST- fusion protein (GST-WLN5-6(G591D). Lane 1 molecular marker, lane 2 and 3 represent enterokinase cleavage using 0.5 and 1 enzyme units respectively.

Wilson Protein Domain 4 (mWD4) - Avitag

The cloned mWD4-Avitag plasmid was obtained from the laboratory of Professor Peng Chen at Cornell University. This plasmid was transformed in Rosetta (DE3) cells and inoculated in LB for protein induction and expression. The overexpressed protein was extracted and purified using anion exchange chromatography and gel filtration. Pure proteins were submitted for mass spectrometry before shipment to Cornell University. mass spectrometry results indicated the correct mass.

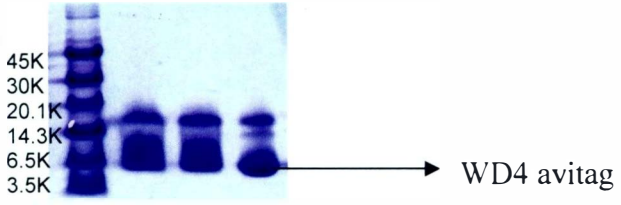

Figure 15: Tricine SDS-PAGE (15%) showing pure fractions of mWD4-Avitag protein. Lane 1; rainbow marker, lanes 2-4 denote different gel filtration fractions. Samples in lanes 3 and 4 were treated with iodoacetamide.

1D (^{1}H) NMR of WLN6

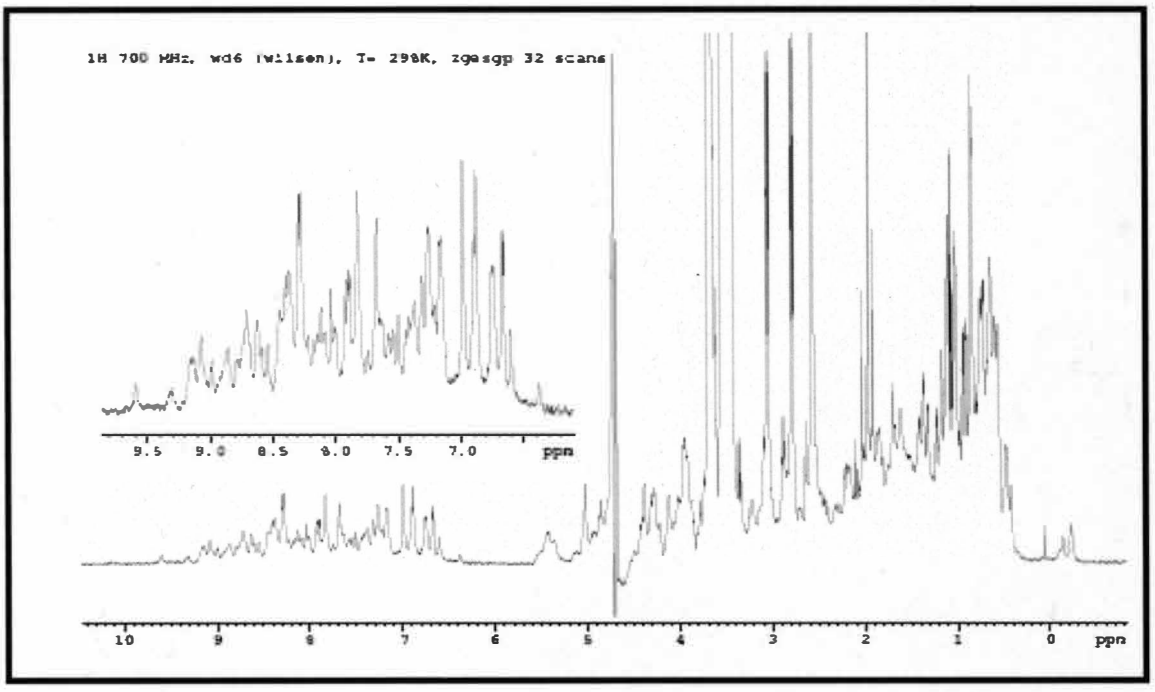

Figure 16. 1D proton NMR of native WLN6: Inset: Expanded spectrum of amide region.

The above NMR data was done at Centre for Magnetic Resonance, University of Florence, Italy using a Bruker 700 MHz NMR machine. The amide region (chemical shifts 5-10) show a good peak distribution and this is an indication of good protein folding (Figure 16). To understand other parameters in terms of protein structures, it was necessary to label the protein with both ^{15}N and ^{13}C.

^{1}H, ^{15}N Hetero Spin Quantum Correlation (HSQC)

The ^{15}N labeled native WLN6 was analyzed for HSQC using Bruker 700 high frequency NMR in CERM, University of Florence. 8 scans were made during the data acquisition. The H,^{15}N WLN6 protein displays broad distribution of NMR frequency also observed in spread-out cross peak signals in the ^{1}H-^{15}N HSQC (Figure 17). Unfolded

proteins normally show heavy overlap of signals on the ^{1}H-^{15}N HSQC spectrum. WLN6 is well folded according to the 2D ^{1}H-^{15}N HSQC spectrum (Figure 17). Assignment of the ^{1}H-^{15}N HSQC spectrum is also consistent with the WLN6 protein sequence and the number of amino acid residues. The distribution of signals is crucial for further structural determination.

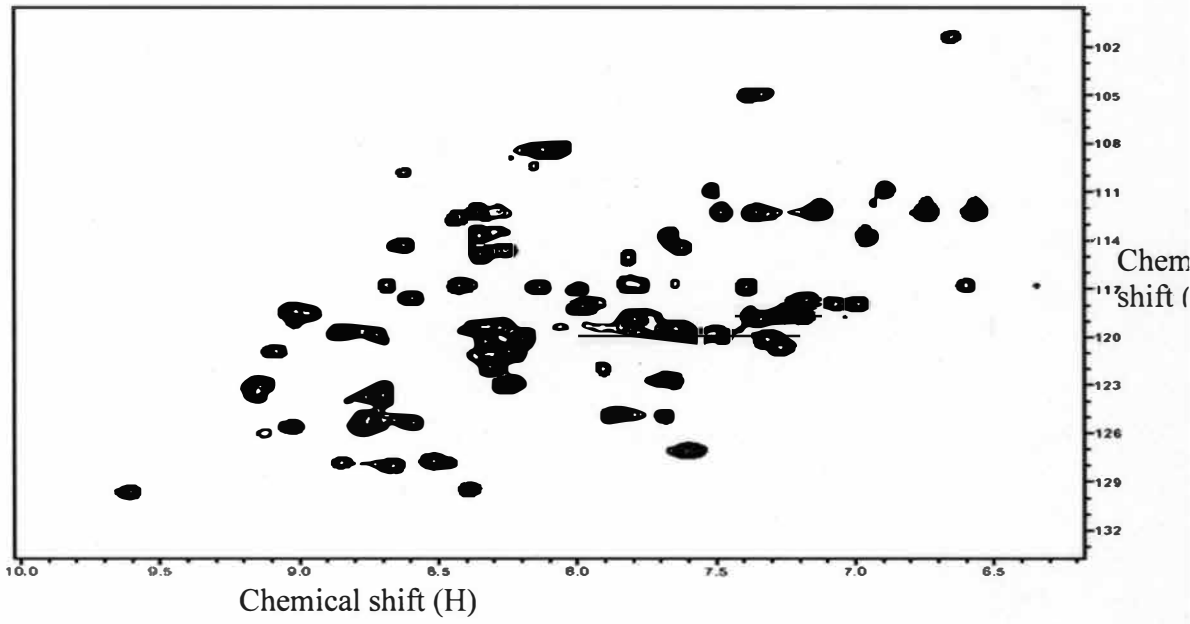

Figure 17. ^{1}H,^{15}N HSQC signals for native WLN6. The cross-distribution of the signals indicates a well-folded protein.

Nuclear Overhauser (NOESY) and TOCSY Experiments

The NOESY signals of a double-labeled WLN6 (^{15}N and ^{13}C-labeled) were acquired alongside HSQC data. The signals were acquired with a Bruker-700 NMR machine at 25°C in 150 ms. The signals obtained are well-distributed and correlates the dipolar interaction of spins and orientation of protons in space (Figure 18). NOESY also correlates protons which are distant in the amino acid sequence but close in space due to tertiary structure. The scalar J coupling constants were calculated and used for structure

calculation. The NOESY signals of the amide region were also acquired (Figure 19) for complete assignment of the backbone signals.

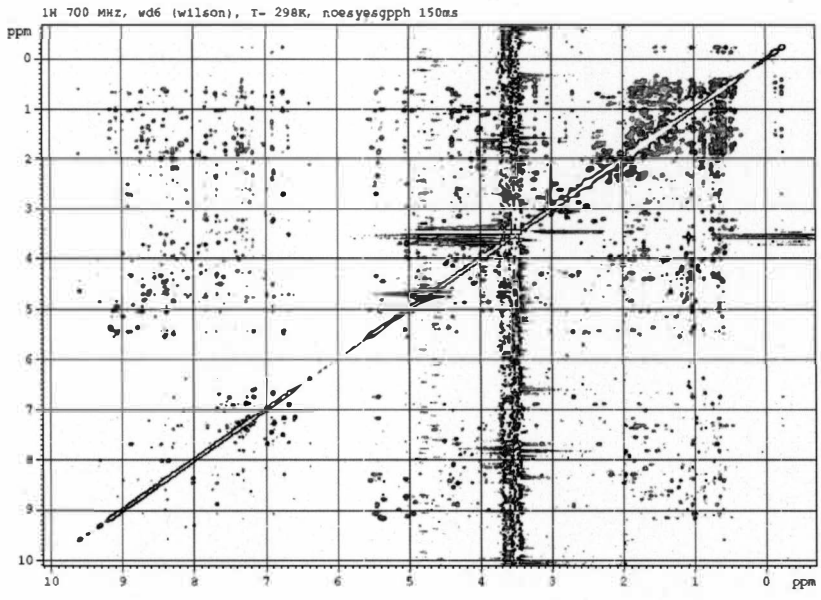

Figure 18: The NOESY signals of WLN6 at 298K.

A TOCSY experiment was also performed for WLN6 using Bruker-700 NMR machine. The data was also acquired at 25°C in 50 ms scans (Figure 20). The signals were also well-dispersed and an indication of well-folded protein. In the TOCSY experiment, magnetization is dispersed over a complete spin system of an amino acid by successive scalar coupling. The TOCSY experiment correlates all protons of a spin system. Thus a characteristic pattern of signals results for each amino acid from which the amino acid can be identified and subsequently assign the peaks. The peak assignments were done manually using signal charts and the CARA computer program.

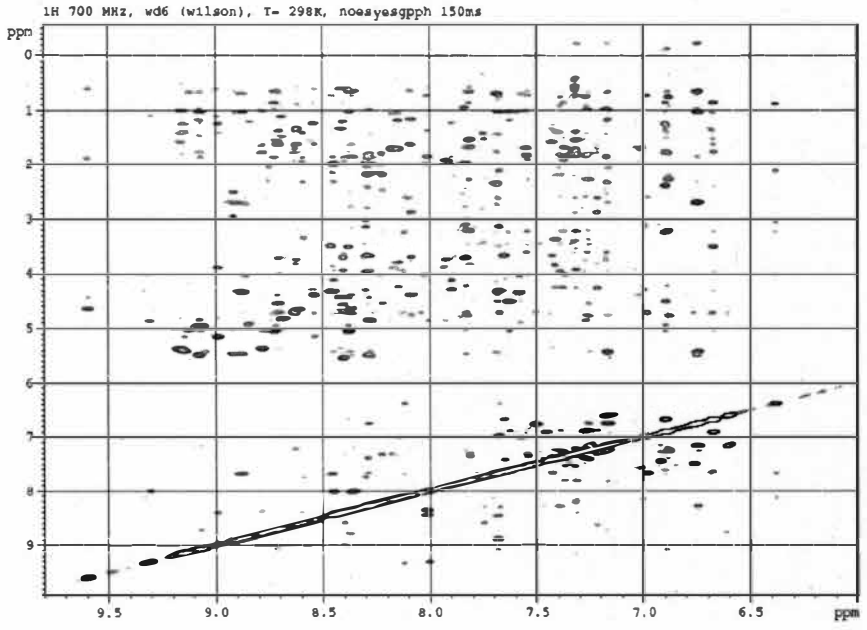

Figure 19. The NOESY signals of the amide region of WLN6.

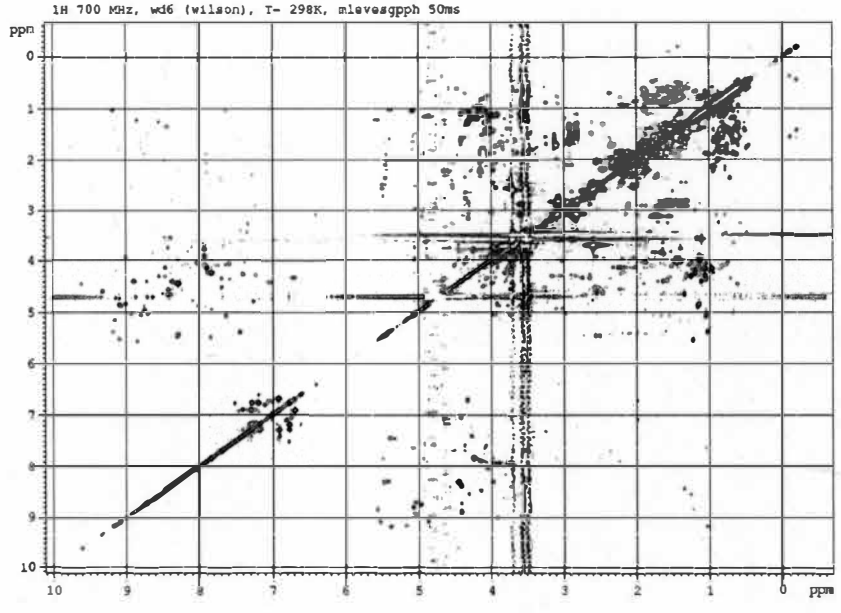

Figure 20: TOCSY signals of WLN6. The experiment was done at a temperature of 298K.

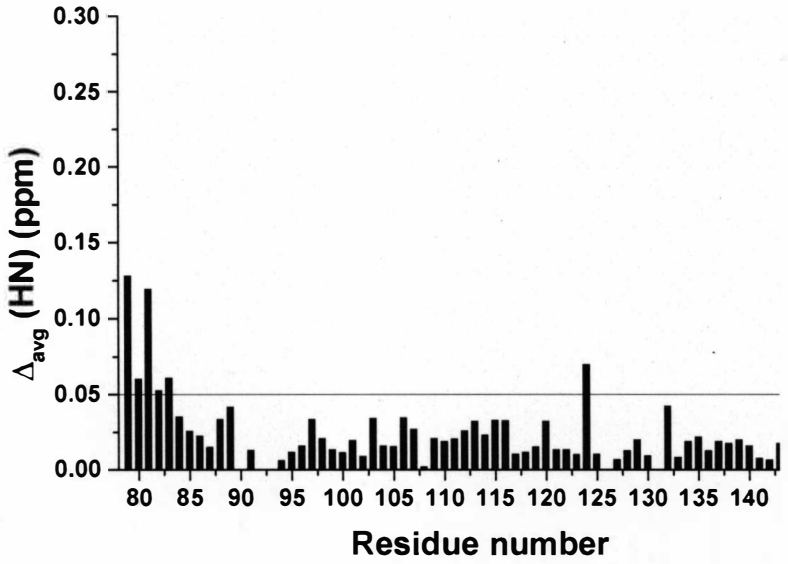

Figure 21: Chemical shift difference (δ_{avg}(HN)) due to superposition of HSQC data for WLN6 and WLN5-6 on amino acid residues 79-146 (with respect to WLN5-6)

Solution NMR structure of WLN6

The secondary structure of WLN6 was determined. The NMR structures of WLN6 and WLN5-6 were compared by mapping the average chemical shifts (δ avg(HN)) of the HSQC data for both proteins. The data indicated that the superimposed signal shifts (δ avg(HN)) were less than 0.05 for majority peaks and therefore insignificant (Figure 21). The structure WLN6 was calculated to be just the same as the domain 6 region of WLN5-6 structure. The solution NMR structure shows that this domain bears a ferrodoxin-like structure, βαββαβ (Figure 22)). An analysis of WLN6 NMR data revealed the following secondary structural elements; β1(81-86), α1(94-103), β2(109-114), β3(119-125), α2(132-140), β4(144-147) (Figure 22)(The residue numbers correspond to domains 5 and 6 together) The Cys 91 and 94 which coordinate copper in this metal binding domain are located in the first loop and first α-helix respectively.

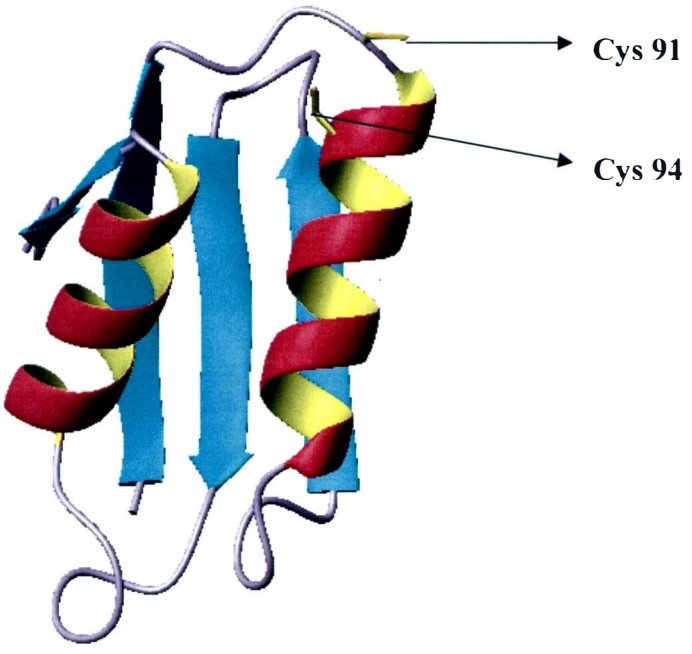

Figure 22: Ribbon-like NMR structure of Wilson protein domain 6. Cys 91 and 94 indicate the cysteine residues involved in binding copper in the CXXC motif. The residue numbers correspond to domains 5 and 6 together.

CHAPTER IV

DISCUSSION

To better understand the disease-causing mutation of Wilson protein domain 6, both native and mutant WLN6 constructs were expressed in vitro. The first step was to obtain the wildtype (native) form of this protein. The sequence of the sixth domain of wildtype ATPB7 gene was amplified by PCR, sub-cloned in pET24d vector, and overexpressed in *E. coli* cells. The expressed protein was extracted from bacterial cells using freeze-thaw extraction method, and then subjected to two purification steps: anion exchange chromatography and size exclusion chromatography (gel filtration). The column used in the anion exchange chromatography was diethylaminoethyl (DEAE). Table 5 shows that majority of soluble cellular proteins bound to the DEAE column after loading and washing steps. WLN6 was expected to bind to the column because the pH of the solvent buffer (20 mM MES/Na, pH 6) was slightly higher than its pI (5.2). Since the column was also run at pH 6, WLN6 would posses an overall negative charge. This would facilitate electrostatic interaction between the protein (negatively charged) and the positively charged diethylaminoethyl therefore WLN6 was retained on the resin. Elution of WLN6 was realized in low salt concentration relative to other proteins which also bound to the column. This suggests the contaminant proteins are more acidic, relative to WLN6 and confirms that the pI of WLN6 is indeed slightly lower than pH 6 (our measured pI of WLN6 is 5.2). While DEAE step initiated the protein purification process, the analytical gel from this purification still confirmed the presence of other contaminant proteins of

higher molecular weight (Figure. 7). These contaminant proteins necessitated the next purification step; gel filtration. In the gel filtration column, WLN6 eluted among the last protein-containing fractions. This shows that the size of this protein is smaller (~7 kD) compared to other proteins as observed in the SDS-PAGE (Figures 7, 9). The results from gel filtration indicate complete purification of WLN6 (Fig. 8). To study the disease-causing mutation, point mutagenesis of the WLN6 native plasmid DNA was carried out.

The mutation, G591D, was successfully introduced and confirmed by DNA sequencing. A time-course induction study of WLN6(G591D) expressed in Rosetta (DE3) cells showed that expression of this protein was positive in millimolar concentrations of IPTG. T7 polymerase then transcribes the mutated gene for domain 6 located on the pET24d vector. Rosetta (DE3) strains of *E. coli* were utilized for protein expression because they contain a chromosomal copy of T7 RNA polymerase, which is inducible by *lac* UV5 promoter. In addition, these strains of cells lack membrane proteases that could potentially degrade proteins (including WLN6) during purification. Figure 10 shows that WLN6(G591D) is inducible by IPTG. However, the mutant WLN6(G591D) was not easily extracted in freeze-thaw extraction buffer (the buffer that easily extracts native WLN6 protein). Several extraction attempts were made by changing the buffer conditions and composition. The protein extraction was still unsuccessful. The bacterial pellets containing the mutant protein were further subjected to sonication but still the extraction was not successful. We finally sought the use of a commercial extraction reagent from Novagen. BugBuster® Protein Extraction Reagent is formulated to gently disrupt the cell wall of *E. coli* and liberate soluble proteins. It

provides a simple, rapid, low-cost alternative to mechanical methods such as French press or sonication for releasing expressed target protein in preparation for purification or other applications. The protein was still not extracted from the pellets even after using this reagent. It was concluded that the mutant protein was an inclusion body and therefore solubilization techniques would be the last preferred method for its extraction. Solubilization of bacterial pellets involves the use of chaotropic agents (urea and guanidine hydrogen chloride) at higher concentration (Arakawa & Timasheff, 1984). A higher concentration of Guanidinium Chloride was used to solubilize bacterial pellets and denature the mutant protein, but when the protein was exchanged in a refolding buffer, it precipitated out in both low and high salt buffers. Another strategy was developed after observing the stability of native WLN5-6 protein with varied concentrations of Guanidinium chloride (GnHCl). Despite being a strong denaturant, WLN5-6 titrated with GnHCl was still stable in up to 3M GnHCl (H,^{15}N-HSQC experiments in Florence, Italy, data unpublished) (Note: Most proteins are completely denatured in 3M GnHCl). With the hypothesis that the native stable WLN5-6 is more stable due to the additional domain 5, a mutant protein also containing domain 5 may also impart stability to the mutant protein, WLN5-6(G591D). Therefore G591D mutation was successfully introduced in the double construct template and the mutagenic plasmid was tested for protein expression. However, the WLN5-6(G591D) protein extraction levels were also insignificant to obtain a desirable amount of protein for NMR studies although little amounts were realized for CD studies.

In another attempt to increase the solubility and expression levels of the mutant WLN5-6(G591), the plasmid was re-cloned in both GST and thioredoxin fusion since the expression levels for fusion proteins are known to be significant. The LIC clones were expressed for the mutant fusion proteins and extracted from the cells successfully. After purification with HisTag and GST columns, both enterokinase and Factor Xa fusion cleavage was performed to isolate the pure mutant proteins. The cleavage was not successful and this led us to question the sequence. The LIC recombinant plasmids were re-submitted for protein sequencing and there was an indication of an insertion of 5 base pairs just after the point of mutation.

^{1}H NMR data of the native WLN6 protein indicates a good protein folding as observed by well-dispersed peaks in both amide (^{1}H chemical shifts 6-10 ppm, Fig 16) and side chain regions (^{1}H chemical shifts 0-3 ppm, Fig 16). The numerous chemical shift peaks seen for amide protons between 6.5-9.5 ppm, for the alpha protons 3-5 ppm and for aliphatic protons 0.5 ppm to 3 ppm is a clear indication that the sample was in a stable condition, optimal for NMR experiments.

To obtain the structure of the native form of WLNP, the protein was expressed in complete minimal media enriched with ^{15}N and ^{13}C to ensure incorporation of these NMR-active elements in the structure of the protein. The use of heteronuclei, ^{15}N and ^{13}C, allows some new features in NMR which facilitate the structure determination. However, their natural abundance and gyromagnetic ratio are markedly lower than that of the proton. Two strategies used to increase the low sensitivity of these nuclei are isotopic enrichment of these nuclei in proteins and enhancement of the signal to noise ratio by the use of inverse NMR experiment in which the magnetization is transferred from protons to the heteronucleus (HSQC). Other reasons for using ^{15}N and ^{13}C to label WLN6 are

because they are not radioactive and therefore harmless and they have a spin of ½ and therefore can only have two quantum energy levels.

The 2D HSQC spectrum of WLN6 (Figure 17) was consistent with the WLN6 amino acid sequence and this was a key step it solving the structure of native WLN6 protein. The 2D HSQC data shows well-dispersed signals and resonance. This shows that WLN6 is well-folded and in stable condition. The sharp dispersed signals on HSQC spectrum is also a good indicator of optimal NMR experiment conditions and the monomeric nature of WLN6. Monomeric proteins show sharp signals on HSQC spectrum. An amino acid residue assignment of all the HSQC signals was done to determine the backbone structure of the protein.

3D NOESY (Figures 18, 19) and TOCSY (Figure 20) experiments were also done to establish the orientation of the side chains and bond angles respectively. The distances derived from nuclear Overhauser effect (NOE) spectra were converted into three-dimensional structures by computer algorithms (CARA program). The native structure of WLN5-6 was also calculated using its HSQC data, NOESY and TOCSY data. Besides these data, the J coupling constraints and the relaxation measurements were also available for native WLN5-6. By mapping the HSQC data of WLN6 to the WLN5-6, we were able to calculate the two-dimensional chemical shift difference these two proteins. The chemical shift difference (δ_{avg}(HN)) of the HSQC signals in WLN6 with respect to WLN5-6 (except amino acid residue 124) was below 0.05. (Figure 20) The chemical shift difference is considered insignificant if below 0.05. However, the first 5 residues (79-83) show a > 0.05 average chemical shift difference and but these values show a decrease towards the 83rd residue. We believe that this is the effect of domain 5 on domain 6

which affects the chemical environment of the first few residues in domain 6 and thus the significant chemical shift difference.

Based on the HSQC assignment, NOESY, TOCSY data and the HSQC mapping, the structure of WLN6 was calculated. WLN6 was resolved to have a ferroxidin-like βαββαβ (Figure 22) which is in agreement with the predicted model (Figure 2). WLN6 structure is monomeric and assumes a similar structure even its multi-construct form. The recently published structure of WLN5-6 (Achila *et al*, 2006) also sheds more light on Wilson protein.

The CD data obtained for mutant protein WLN5-6(G591D) indicates that the number of α- helices constitute a one-third fraction of the entire motif. This may indicate that the overall βαββαβ is still maintained in the mutant protein, WLN6(G591D). The NMR structure of native WLN6 indicates that Glycine 591(mutated to D in mutant protein) is situated at the protein loop at the beginning in the beginning of the second β-sheet. This mutation could possibly hinder the flexibility of the protein loop rendering the mutant protein unstable with subsequent low solubility which might hinder the normal function of the protein. In a similar study of A629P mutant of Menkes protein, a WLNP homologue, (Banci *et al*, 2005), the authors suggest that the mutation makes the protein beta sheet more solvent accessible, possibly resulting in an enhanced susceptibility of ATP7A to proteolytic cleavage and/or in reduced capability of Cu^{+} translocation. This similar mechanism may be in play in this mutation since the mutation is situated at the beginning of the beta sheet. To validate this fact, an NMR solution structure of this mutant protein should be resolved. To understand why this apparently minor amino acid replacement is pathogenic, the solution structures and dynamics on various time-scales of

wild-type and WLN6(G591D) should be determined both in the apo- and Cu^{+}-loaded forms. The interaction in vitro with the physiological ATP7B copper (I)-donor (HAH1) should be additionally studied.

Conclusion

We have cloned, expressed and purified the native form of WLN6. We have expressed the disease-causing mutant protein as a 2-domain construct WLN5-6(G591D). The CD data of these two proteins predict an α-helicity of 23%. The solution NMR structure of the native WLN6 reveals a monomer with a βαββαβ ferroxidin-like fold. We propose that the mutant form of this protein, WLN6(G591D), may have a similar overall fold to the native protein based on the CD data. This is also consistent with the recently published mutant domain 6 (MKL6(A629B) structure of an analogous protein, MNKP (Banci & Bertini & Cantini & Migliardi *et al.*, 2005). In addition we propose a similar mechanism in copper-uptake impairment between these two mutant proteins based on the position of both mutations.

BIBLIOGRAPHY

Achila, D., Banci, L., Bertini, I., Bunce, J., Ciofi-Baffoni, S. & Huffman, D. L. (2006). Structure of human wilson protein domains 5 and 6 and their interplay with domain 4 and the copper chaperone hah1 in copper uptake. *Proc Natl Acad Sci U S A. 103*, 5729-5734.

Arakawa, T. & Timasheff, S. N. (1984). Protein stabilization and destabilization by guanidinium salts. *Biochemistry. 23*, 5924-5929.

Arnesano, F., Banci, L., Bertini, I., Cantini, F., Ciofi-Baffoni, S., Huffman, D. L. & O'Halloran, T. V. (2001). Characterization of the binding interface between the copper chaperone atx1 and the first cytosolic domain of ccc2 atpase. *J Biol Chem. 276*, 41365-41376.

Arnesano, F., Banci, L., Bertini, I., Ciofi-Baffoni, S., Molteni, E., Huffman, D. L. & O'Halloran, T. V. (2002). Metallochaperones and metal-transporting atpases: A comparative analysis of sequences and structures. *Genome Res. 12*, 255-271.

Banci, L., Bertini, I., Ciofi-Baffoni, S., Huffman, D. L. & O'Halloran, T. V. (2001). Solution structure of the yeast copper transporter domain ccc2a in the apo and cu(i)-loaded states. *J Biol Chem. 276*, 8415-8426.

Banci, L., Bertini, I., Del Conte, R., D'Onofrio, M. & Rosato, A. (2004). Solution structure and backbone dynamics of the cu(i) and apo forms of the second metal-binding domain of the menkes protein atp7a. *Biochemistry. 43*, 3396-3403.

Banci, L., Bertini, I., Cantini, F., Chasapis, C. T., Hadjiliadis, N. & Rosato, A. (2005). A nmr study of the interaction of a three-domain construct of atp7a with copper(i) and copper(i)-hah1: The interplay of domains. *J Biol Chem. 280*, 38259-38263.

Banci, L., Bertini, I., Cantini, F., Migliardi, M., Rosato, A. & Wang, S. (2005). An atomic-level investigation of the disease-causing a629p mutant of the menkes protein, atp7a. *J Mol Biol. 352*, 409-417.

Banci, L., Bertini, I., Ciofi-Baffoni, S., Chasapis, C. T., Hadjiliadis, N. & Rosato, A. (2005). An nmr study of the interaction between the human copper(i) chaperone and the second and fifth metal-binding domains of the menkes protein. *Febs J. 272*, 865-871.

Banci, L., Bertini, I., Cantini, F., DellaMalva, N., Herrmann, T., Rosato, A. & Wuthrich, K. (2006). Solution structure and intermolecular interactions of the third metal-binding domain of atp7a, the menkes disease protein. *J Biol Chem. 281*, 29141-29147.

Banci, L., Bertini, I., Cantini, F., Felli, I. C., Gonnelli, L., Hadjiliadis, N., Pierattelli, R., Rosato, A. & Voulgaris, P. (2006). The atx1-ccc2 complex is a metal-mediated protein-protein interaction. *Nat Chem Biol. 2*, 367-368.

Bayer, T. A., Schafer, S., Simons, A., Kemmling, A., Kamer, T., Tepest, R., Eckert, A., Schussel, K., Eikenberg, O., Sturchler-Pierrat, C., Abramowski, D., Staufenbiel, M. & Multhaup, G. (2003). Dietary cu stabilizes brain superoxide dismutase 1 activity and reduces amyloid abeta production in app23 transgenic mice. *Proc Natl Acad Sci U S A. 100*, 14187-14192.

Bertinato, J., Iskandar, M. & L'Abbe, M. R. (2003). Copper deficiency induces the upregulation of the copper chaperone for cu/zn superoxide dismutase in weanling male rats. *J Nutr. 133*, 28-31.

Bertinato, J. & L'Abbe, M. R. (2003). Copper modulates the degradation of copper chaperone for cu,zn superoxide dismutase by the 26 s proteosome. *J Biol Chem. 278*, 35071-35078.

Brewer, G. J. & Yuzbasiyan-Gurkan, V. (1992). Wilson disease. *Medicine (Baltimore). 71*, 139-164.

Brewer, G. J., Hedera, P., Kluin, K. J., Carlson, M., Askari, F., Dick, R. B., Sitterly, J. & Fink, J. K. (2003). Treatment of wilson disease with ammonium tetrathiomolybdate: Iii. Initial therapy in a total of 55 neurologically affected patients and follow-up with zinc therapy. *Arch Neurol. 60*, 379-385.

Bull, P. C., Thomas, G. R., Rommens, J. M., Forbes, J. R. & Cox, D. W. (1993). The wilson disease gene is a putative copper transporting p-type atpase similar to the menkes gene. *Nat Genet. 5*, 327-337.

Bull, P. C. & Cox, D. W. (1994). Wilson disease and menkes disease: New handles on heavy-metal transport. *Trends Genet. 10*, 246-252.

Casareno, R. L., Waggoner, D. & Gitlin, J. D. (1998). The copper chaperone ccs directly interacts with copper/zinc superoxide dismutase. *J Biol Chem. 273*, 23625-23628.

Cater, M. A., Forbes, J., La Fontaine, S., Cox, D. & Mercer, J. F. (2004). Intracellular trafficking of the human wilson protein: The role of the six n-terminal metal-binding sites. *Biochem J. 380*, 805-813.

Christodoulou, J., Danks, D. M., Sarkar, B., Baerlocher, K. E., Casey, R., Horn, N., Tumer, Z. & Clarke, J. T. (1998). Early treatment of menkes disease with parenteral copper-histidine: Long-term follow-up of four treated patients. *Am J Med Genet. 76*, 154-164.

Cobine, P. A., Pierrel, F., Bestwick, M. L. & Winge, D. R. (2006). Mitochondrial matrix copper complex used in metallation of cytochrome oxidase and superoxide dismutase. *J Biol Chem. 281*, 36552-36559.

Cox, D. W. (1996). Molecular advances in wilson disease. *Prog Liver Dis. 14*, 245-264.

Cox, D. W., Prat, L., Walshe, J. M., Heathcote, J. & Gaffney, D. (2005). Twenty-four novel mutations in wilson disease patients of predominantly european ancestry. *Hum Mutat. 26*, 280.

Coyle, P., Philcox, J. C., Carey, L. C. & Rofe, A. M. (2002). Metallothionein: The multipurpose protein. *Cell Mol Life Sci. 59*, 627-647.

Culotta, V. C., Klomp, L. W., Strain, J., Casareno, R. L., Krems, B. & Gitlin, J. D. (1997). The copper chaperone for superoxide dismutase. *J Biol Chem. 272*, 23469-23472.

Culotta, V. C. & Gitlin, J. D. (2001). "Disorders of copper transport" in The molecular and metabolic basis of inherited disease, (R., S.C., L., B.A. and S., S.W., eds.) McGraw-Hill, New York, pp. 3105-3136.

Cumings, J. N. (1948). The copper and iron content of brain and liver in the normal and in hepato-lenticular degeneration. *Brain. 71*, 410-415.

Cuthbert, J. A. (1998). Wilson's disease. Update of a systemic disorder with protean manifestations. *Gastroenterol Clin North Am. 27*, 655-681, vi-vii.

Danks, D. M. (1980). Copper deficiency in humans. *Ciba Found Symp. 79*, 209-225.

Danks, D. M. (1995). "Disorders of copper transport " in The metabolic and molecular basis of inherited disease, 7th ed., (Scriver, C.R., Beaudet, A.L., Sly, W.M. and Valle, D., eds.) McGraw-Hill, New York, pp. 2211.

de Silva, D., Davis-Kaplan, S., Fergestad, J. & Kaplan, J. (1997). Purification and characterization of fet3 protein, a yeast homologue of ceruloplasmin. *J Biol Chem. 272*, 14208-14213.

DiDonato, M., Narindrasorasak, S., Forbes, J. R., Cox, D. W. & Sarkar, B. (1997). Expression, purification, and metal binding properties of the n-terminal domain from the wilson disease putative copper-transporting atpase (atp7b). *J Biol Chem. 272*, 33279-33282.

DiDonato, M., Hsu, H. F., Narindrasorasak, S., Que, L., Jr. & Sarkar, B. (2000). Copper-induced conformational changes in the n-terminal domain of the wilson disease copper-transporting atpase. *Biochemistry. 39*, 1890-1896.

DiDonato, M., Zhang, J. Y., Que, L. & Sarkar, B. (2002). Zinc binding to the nh2-terminal domain of the wilson disease copper-transporting atpase - implications for in vivo metal ion-mediated regulation of atpase activity. *Journal of Biological Chemistry. 277*, 13409-13414.

DiGuiseppi, J. & Fridovich, I. (1984). The toxicology of molecular oxygen. *Crit Rev Toxicol. 12*, 315-342.

Dmitriev, O., Tsivkovskii, R., Abildgaard, F., Morgan, C. T., Markley, J. L. & Lutsenko, S. (2006). Solution structure of the n-domain of wilson disease protein: Distinct nucleotide-binding environment and effects of disease mutations. *Proc Natl Acad Sci U S A. 103*, 5302-5307.

Failla, M. L., Johnson, M. A. & Prohaska, J. R. (2001). "Copper" in Present knowledge in nutrition, 8th ed., (Bowman, B.A. and Russell, R.M., eds.) ILSI Press, Washington, D. C., pp. 373-383.

Farrow, N. A., Zhang, O., Szabo, A., Torchia, D. A. & Kay, L. E. (1995). Spectral density function mapping using 15n relaxation data exclusively. *J Biomol NMR. 6*, 153-162.

Fatemi, N. & Sarkar, B. (2002). Structural and functional insights of wilson disease copper-transporting atpase. *Journal of Bioenergetics and Biomembranes. 34*, 339-349.

Forbes, J. R., Hsi, G. & Cox, D. W. (1999). Role of the copper-binding domain in the copper transport function of atp7b, the p-type atpase defective in wilson disease. *J Biol Chem. 274*, 12408-12413.

Fox, P. L. (2003). The copper-iron chronicles: The story of an intimate relationship. *Biometals. 16*, 9-40.

Frommer, D. J. (1974). Defective biliary excretion of copper in wilson's disease. *Gut. 15*, 125-129.

Frydman, M., Bonne-Tamir, B., Farrer, L. A., Conneally, P. M., Magazanik, A., Ashbel, S. & Goldwitch, Z. (1985). Assignment of the gene for wilson disease to chromosome 13: Linkage to the esterase d locus. *Proc Natl Acad Sci U S A. 82*, 1819-1821.

Gitlin, J. D. (2003). Wilson disease. *Gastroenterology. 125*, 1868-1877.

Gitschier, J., Moffat, B., Reilly, D., Wood, W. I. & Fairbrother, W. J. (1998). Solution structure of the fourth metal-binding domain from the menkes copper-transporting atpase. *Nat Struct Biol. 5*, 47-54.

Gollan, J. L. & Gollan, T. J. (1998). Wilson disease in 1998: Genetic, diagnostic and therapeutic aspects. *J Hepatol. 28 Suppl 1*, 28-36.

Gu, M., Cooper, J. M., Butler, P., Walker, A. P., Mistry, P. K., Dooley, J. S. & Schapira, A. H. (2000). Oxidative-phosphorylation defects in liver of patients with wilson's disease. *Lancet. 356*, 469-474.

Guo, Y., Nyasae, L., Braiterman, L. T. & Hubbard, A. L. (2005). Nh2-terminal signals in atp7b cu-atpase mediate its cu-dependent anterograde traffic in polarized hepatic cells. *Am J Physiol Gastrointest Liver Physiol. 289*, G904-916.

Hamza, I., Schaefer, M., Klomp, L. W. & Gitlin, J. D. (1999). Interaction of the copper chaperone hah1 with the wilson disease protein is essential for copper homeostasis. *Proc Natl Acad Sci U S A. 96*, 13363-13368.

Hamza, I., Faisst, A., Prohaska, J., Chen, J., Gruss, P. & Gitlin, J. D. (2001). The metallochaperone atox1 plays a critical role in perinatal copper homeostasis. *Proc Natl Acad Sci U S A. 98*, 6848-6852.

Huffman, D. L. & O'Halloran, T. V. (2000). Energetics of copper trafficking between the atx1 metallochaperone and the intracellular copper transporter, ccc2. *J Biol Chem. 275*, 18611-18614.

Huffman, D. L. & O'Halloran, T. V. (2001). Function, structure, and mechanism of intracellular copper trafficking proteins. *Annu Rev Biochem. 70*, 677-701.

Hung, I. H., Suzuki, M., Yamaguchi, Y., Yuan, D. S., Klausner, R. D. & Gitlin, J. D. (1997). Biochemical characterization of the wilson disease protein and functional expression in the yeast saccharomyces cerevisiae. *J Biol Chem. 272*, 21461-21466.

Hung, Y. H., Layton, M. J., Voskoboinik, I., Mercer, J. F. & Camakaris, J. (2007). Purification and membrane reconstitution of catalytically active menkes copper-transporting p-type atpase (mnk; atp7a). *Biochem J. 401*, 569-579.

Huster, D. & Lutsenko, S. (2003). The distinct roles of the n-terminal copper-binding sites in regulation of catalytic activity of the wilson's disease protein. *J Biol Chem. 278*, 32212-32218.

Iida, M., Terada, K., Sambongi, Y., Wakabayashi, T., Miura, N., Koyama, K., Futai, M. & Sugiyama, T. (1998). Analysis of functional domains of wilson disease protein (atp7b) in saccharomyces cerevisiae. *FEBS Lett. 428*, 281-285.

Jensen, P. Y., Bonander, N., Horn, N., Tumer, Z. & Farver, O. (1999). Expression, purification and copper-binding studies of the first metal-binding domain of menkes protein. *European Journal of Biochemistry. 264*, 890-896.

Jensen, P. Y., Bonander, N., Moller, L. B. & Farver, O. (1999). Cooperative binding of copper(i) to the metal binding domains in menkes disease protein. *Biochim Biophys Acta. 1434*, 103-113.

Kelner, G. S., Lee, M., Clark, M. E., Maciejewski, D., McGrath, D., Rabizadeh, S., Lyons, T., Bredesen, D., Jenner, P. & Maki, R. A. (2000). The copper transport protein atox1 promotes neuronal survival. *J Biol Chem. 275*, 580-584.

Klomp, A. E., van de Sluis, B., Klomp, L. W. & Wijmenga, C. (2003). The ubiquitously expressed murr1 protein is absent in canine copper toxicosis. *J Hepatol. 39*, 703-709.

Klomp, L. W., Lin, S. J., Yuan, D. S., Klausner, R. D., Culotta, V. C. & Gitlin, J. D. (1997). Identification and functional expression of hah1, a novel human gene involved in copper homeostasis. *J Biol Chem. 272*, 9221-9226.

Kong, G. K., Adams, J. J., Harris, H. H., Boas, J. F., Curtain, C. C., Galatis, D., Masters, C. L., Barnham, K. J., McKinstry, W. J., Cappai, R. & Parker, M. W. (2007). Structural studies of the alzheimer's amyloid precursor protein copper-binding domain reveal how it binds copper ions. *J Mol Biol. 367*, 148-161.

Kuo, Y. M., Zhou, B., Cosco, D. & Gitschier, J. (2001). The copper transporter ctr1 provides an essential function in mammalian embryonic development. *Proc Natl Acad Sci U S A. 98*, 6836-6841.

Larin, D., Mekios, C., Das, K., Ross, B., Yang, A. S. & Gilliam, T. C. (1999). Characterization of the interaction between the wilson and menkes disease proteins and the cytoplasmic copper chaperone, hah1p. *J Biol Chem. 274*, 28497-28504.

Lee, J., Pena, M. M., Nose, Y. & Thiele, D. J. (2002). Biochemical characterization of the human copper transporter ctr1. *J Biol Chem. 277*, 4380-4387.

Lin, S. J. & Culotta, V. C. (1995). The atx1 gene of saccharomyces cerevisiae encodes a small metal homeostasis factor that protects cells against reactive oxygen toxicity. *Proc Natl Acad Sci U S A. 92*, 3784-3788.

Lin, S. J., Pufahl, R. A., Dancis, A., O'Halloran, T. V. & Culotta, V. C. (1997). A role for the saccharomyces cerevisiae atx1 gene in copper trafficking and iron transport. *J Biol Chem. 272*, 9215-9220.

Loudianos, G., Dessi, V., Lovicu, M., Angius, A., Nurchi, A., Sturniolo, G. C., Marcellini, M., Zancan, L., Bragetti, P., Akar, N., Yagci, R., Vegnente, A., Cao, A. & Pirastu, M. (1998). Further delineation of the molecular pathology of wilson disease in the mediterranean population. *Hum Mutat. 12*, 89-94.

Lutsenko, S. & Kaplan, J. H. (1995). Organization of p-type atpases: Significance of structural diversity. *Biochemistry. 34*, 15607-15613.

Lutsenko, S., Petrukhin, K., Cooper, M. J., Gilliam, C. T. & Kaplan, J. H. (1997). N-terminal domains of human copper-transporting adenosine triphosphatases (the wilson's and menkes disease proteins) bind copper selectively in vivo and in vitro with stoichiometry of one copper per metal-binding repeat. *J Biol Chem. 272*, 18939-18944.

Lutsenko, S. & Petris, M. J. (2003). Function and regulation of the mammalian copper-transporting atpases: Insights from biochemical and cell biological approaches. *J Membr Biol. 191*, 1-12.

Maynard, C. J., Cappai, R., Volitakis, I., Cherny, R. A., White, A. R., Beyreuther, K., Masters, C. L., Bush, A. I. & Li, Q. X. (2002). Overexpression of alzheimer's disease amyloid-beta opposes the age-dependent elevations of brain copper and iron. *J Biol Chem. 277*, 44670-44676.

Menkes, J. H., Alter, M., Steigleder, G. K., Weakley, D. R. & Sung, J. H. (1962). A sex-linked recessive disorder with retardation of growth, peculiar hair, and focal cerebral and cerebellar degeneration. *Pediatrics. 29*, 764-779.

Mitra, B. & Sharma, R. (2001). The cysteine-rich amino-terminal domain of znta, a pb(ii)/zn(ii)/cd(ii)-translocating atpase from escherichia coli, is not essential for its function. *Biochemistry. 40*, 7694-7699.

Monty, J. F., Llanos, R. M., Mercer, J. F. & Kramer, D. R. (2005). Copper exposure induces trafficking of the menkes protein in intestinal epithelium of atp7a transgenic mice. *J Nutr. 135*, 2762-2766.

Moore, S. D. & Cox, D. W. (2002). Expression in mouse kidney of membrane copper transporters atp7a and atp7b. *Nephron. 92*, 629-634.

Payne, A. S., Kelly, E. J. & Gitlin, J. D. (1998). Functional expression of the wilson disease protein reveals mislocalization and impaired copper-dependent trafficking of the common h1069q mutation. *Proc Natl Acad Sci U S A. 95*, 10854-10859.

Pedersen, P. L. & Carafoli, E. (1987). Ion motive atpases.1. Ubiquity, properties, and significance to cell-function. *Trends in Biochemical Sciences. 12*, 146-150.

Peng, J. W. & Wagner, G. (1992). Mapping of the spectral densities of n-h bond motions in eglin c using heteronuclear relaxation experiments. *Biochemistry. 31*, 8571-8586.

Portnoy, M. E., Rosenzweig, A. C., Rae, T., Huffman, D. L., O'Halloran, T. V. & Culotta, V. C. (1999). Structure-function analyses of the atx1 metallochaperone. *J Biol Chem. 274*, 15041-15045.

Prohaska, J. R. (1988). "Biochemical functions of copper in animals" in Essential and toxic trace elements in human health and disease, (Prasad, A.S., ed.), New York, pp. 105-124.

Prohaska, J. R., Geissler, J., Brokate, B. & Broderius, M. (2003). Copper, zinc-superoxide dismutase protein but not mrna is lower in copper-deficient mice and mice lacking the copper chaperone for superoxide dismutase. *Exp Biol Med (Maywood). 228*, 959-966.

Prohaska, J. R. & Gybina, A. A. (2004). Intracellular copper transport in mammals. *J Nutr. 134*, 1003-1006.

Pufahl, R. A., Singer, C. P., Peariso, K. L., Lin, S. J., Schmidt, P. J., Fahrni, C. J., Culotta, V. C., Penner-Hahn, J. E. & O'Halloran, T. V. (1997). Metal ion chaperone function of the soluble cu(i) receptor atx1. *Science. 278*, 853-856.

Puig, S., Lee, J., Lau, M. & Thiele, D. J. (2002). Biochemical and genetic analyses of yeast and human high affinity copper transporters suggest a conserved mechanism for copper uptake. *J Biol Chem. 277*, 26021-26030.

Rae, T. D., Schmidt, P. J., Pufahl, R. A., Culotta, V. C. & O'Halloran, T. V. (1999). Undetectable intracellular free copper: The requirement of a copper chaperone for superoxide dismutase. *Science. 284*, 805-808.

Ralle, M., Lutsenko, S. & Blackburn, N. J. (2003). X-ray absorption spectroscopy of the copper chaperone hah1 reveals a linear two-coordinate cu(i) center capable of adduct formation with exogenous thiols and phosphines. *Journal of Biological Chemistry. 278*, 23163-23170.

Ralle, M., Lutsenko, S. & Blackburn, N. J. (2004). Copper transfer to the n-terminal domain of the wilson disease protein (atp7b): X-ray absorption spectroscopy of reconstituted and chaperone-loaded metal binding domains and their interaction with exogenous ligands. *Journal of Inorganic Biochemistry. 98*, 765-774.

Rosenzweig, A. C., Huffman, D. L., Hou, M. Y., Wernimont, A. K., Pufahl, R. A. & O'Halloran, T. V. (1999). Crystal structure of the atx1 metallochaperone protein at 1.02 a resolution. *Structure. 7*, 605-617.

Rosenzweig, A. C. (2001). Copper delivery by metallochaperone proteins. *Acc Chem Res. 34*, 119-128.

Schaefer, M. & Gitlin, J. D. (1999). Genetic disorders of membrane transport. Iv. Wilson's disease and menkes disease. *Am J Physiol. 276*, G311-314.

Scheinberg, I. H. & Gitlin, D. (1952). Deficiency of ceruloplasmin in patients with hepatolenticular degeneration (wilson's disease). *Science. 116*, 484-485.

Schmidt, P. J., Rae, T. D., Pufahl, R. A., Hamma, T., Strain, J., O'Halloran, T. V. & Culotta, V. C. (1999). Multiple protein domains contribute to the action of the copper chaperone for superoxide dismutase. *J Biol Chem. 274*, 23719-23725.

Solioz, M. & Vulpe, C. (1996). Cpx-type atpases: A class of p-type atpases that pump heavy metals. *Trends Biochem Sci. 21*, 237-241.

Sternlieb, I. (1984). Wilson's disease: Indications for liver transplants. *Hepatology. 4*, 15S-17S.

Sturtz, L. A., Diekert, K., Jensen, L. T., Lill, R. & Culotta, V. C. (2001). A fraction of yeast cu,zn-superoxide dismutase and its metallochaperone, ccs, localize to the intermembrane space of mitochondria. A physiological role for sod1 in guarding against mitochondrial oxidative damage. *J Biol Chem. 276*, 38084-38089.

Suzuki, K. T., Someya, A., Komada, Y. & Ogra, Y. (2002). Roles of metallothionein in copper homeostasis: Responses to cu-deficient diets in mice. *J Inorg Biochem. 88*, 173-182.

Tanzi, R. E., Petrukhin, K., Chernov, I., Pellequer, J. L., Wasco, W., Ross, B., Romano, D. M., Parano, E., Pavone, L., Brzustowicz, L. M. & et al. (1993). The wilson disease gene is a copper transporting atpase with homology to the menkes disease gene. *Nat Genet. 5*, 344-350.

Tao, T. Y. & Gitlin, J. D. (2003). Hepatic copper metabolism: Insights from genetic disease. *Hepatology. 37*, 1241-1247.

Tao, T. Y., Liu, F., Klomp, L., Wijmenga, C. & Gitlin, J. D. (2003). The copper toxicosis gene product murr1 directly interacts with the wilson disease protein. *J Biol Chem. 278*, 41593-41596.

Terada, K., Nakako, T., Yang, X. L., Iida, M., Aiba, N., Minamiya, Y., Nakai, M., Sakaki, T., Miura, N. & Sugiyama, T. (1998). Restoration of holoceruloplasmin synthesis in lec rat after infusion of recombinant adenovirus bearing wnd cdna. *J Biol Chem. 273*, 1815-1820.

Toyoshima, C., Nakasako, M., Nomura, H. & Ogawa, H. (2000). Crystal structure of the calcium pump of sarcoplasmic reticulum at 2.6 a resolution. *Nature. 405*, 647-655.

Toyoshima, C. & Nomura, H. (2002). Structural changes in the calcium pump accompanying the dissociation of calcium. *Nature. 418*, 605-611.

Toyoshima, C. & Mizutani, T. (2004). Crystal structure of the calcium pump with a bound atp analogue. *Nature. 430*, 529-535.

Trumbo, P., Yates, A. A., Schlicker, S. & Poos, M. (2001). Dietary reference intakes: Vitamin a, vitamin k, arsenic, boron, chromium, copper, iodine, iron, manganese, molybdenum, nickel, silicon, vanadium, and zinc. *J Am Diet Assoc. 101*, 294-301.

Tsay, M. J., Fatemi, N., Narindrasorasak, S., Forbes, J. R. & Sarkar, B. (2004). Identification of the "missing domain" of the rat copper-transporting atpase atp7b: Insight into the structural and metal binding characteristics of its n-terminal copper-binding domain. *Biochimica Et Biophysica Acta-Molecular Basis of Disease. 1688*, 78-85.

Tsivkovskii, R., Eisses, J. F., Kaplan, J. H. & Lutsenko, S. (2002). Functional properties of the copper-transporting atpase atp7b (the wilson's disease protein) expressed in insect cells. *J Biol Chem. 277*, 976-983.

Tsivkovskii, R., Efremov, R. G. & Lutsenko, S. (2003). The role of the invariant his-1069 in folding and function of the wilson's disease protein, the human copper-transporting atpase atp7b. *J Biol Chem. 278*, 13302-13308.

van Dongen, E. M., Klomp, L. W. & Merkx, M. (2004). Copper-dependent protein-protein interactions studied by yeast two-hybrid analysis. *Biochem Biophys Res Commun. 323*, 789-795.

Vanderwerf, S. M., Cooper, M. J., Stetsenko, I. V. & Lutsenko, S. (2001). Copper specifically regulates intracellular phosphorylation of the wilson's disease protein, a human copper-transporting atpase. *J Biol Chem. 276*, 36289-36294.

Voskoboinik, I., Mar, J., Strausak, D. & Camakaris, J. (2001). The regulation of catalytic activity of the menkes copper-translocating p-type atpase. Role of high affinity copper-binding sites. *J Biol Chem. 276*, 28620-28627.

Walker, J. M., Tsivkovskii, R. & Lutsenko, S. (2002). Metallochaperone atox1 transfers copper to the nh2-terminal domain of the wilson's disease protein and regulates its catalytic activity. *J Biol Chem. 277*, 27953-27959.

Walker, J. M., Huster, D., Ralle, M., Morgan, C. T., Blackburn, N. J. & Lutsenko, S. (2004). The n-terminal metal-binding site 2 of the wilson's disease protein plays a key role in the transfer of copper from atox1. *Journal of Biological Chemistry. 279*, 15376-15384.

Walter, U., Krolikowski, K., Tarnacka, B., Benecke, R., Czlonkowska, A. & Dressler, D. (2005). Sonographic detection of basal ganglia lesions in asymptomatic and symptomatic wilson disease. *Neurology. 64*, 1726-1732.

Wernimont, A. K., Yatsunyk, L. A. & Rosenzweig, A. C. (2004). Binding of copper(i) by the wilson disease protein and its copper chaperone. *J Biol Chem. 279*, 12269-12276.

White, A. R., Reyes, R., Mercer, J. F., Camakaris, J., Zheng, H., Bush, A. I., Multhaup, G., Beyreuther, K., Masters, C. L. & Cappai, R. (1999). Copper levels are increased in the cerebral cortex and liver of app and aplp2 knockout mice. *Brain Res. 842*, 439-444.

Wilson, S. A. K. (1912). Progressive lenticular degeneration: A familial nervous disease associated with cirrhosis of the liver. *Brain. 34*, 295-507.

Wong, P. C., Waggoner, D., Subramaniam, J. R., Tessarollo, L., Bartnikas, T. B., Culotta, V. C., Price, D. L., Rothstein, J. & Gitlin, J. D. (2000). Copper chaperone for superoxide dismutase is essential to activate mammalian cu/zn superoxide dismutase. *Proc Natl Acad Sci U S A. 97*, 2886-2891.

Wu, J., Forbes, J. R., Chen, H. S. & Cox, D. W. (1994). The lec rat has a deletion in the copper transporting atpase gene homologous to the wilson disease gene. *Nat Genet. 7*, 541-545.

Yamaguchi, Y., Heiny, M. E., Shimizu, N., Aoki, T. & Gitlin, J. D. (1994). Expression of the wilson disease gene is deficient in the long-evans cinnamon rat. *Biochem J. 301 (Pt 1)*, 1-4.

Yang, X. L., Miura, N., Kawarada, Y., Terada, K., Petrukhin, K., Gilliam, T. & Sugiyama, T. (1997). Two forms of wilson disease protein produced by alternative splicing are localized in distinct cellular compartments. *Biochem J. 326 (Pt 3)*, 897-902.

Yatsunyk, L. A. & Rosenzweig, A. C. (2007). Copper(i) binding and transfer by the n-terminus of the wilson disease protein. *J Biol Chem.*

Yuan, D. S., Stearman, R., Dancis, A., Dunn, T., Beeler, T. & Klausner, R. D. (1995). The menkes/wilson disease gene homologue in yeast provides copper to a ceruloplasmin-like oxidase required for iron uptake. *Proc Natl Acad Sci U S A. 92*, 2632-2636.